# The effects of triglycerides and fatty acids on T cells: role in atherosclerosis

Reilly, N.A.

CHAPTER 4

# EPA induces anti-inflammatory transcriptomics in T cells, implicating a triglyceride-independent pathway for cardiovascular risk reduction

**Nathalie A. Reilly**[1,2], Koen F. Dekkers[1], Jeroen Molenaar[1], Sinthuja Arumugam[1], Thomas B. Kuipers[1,3], Yavuz Ariyurek[4], Marten A. Hoeksema[5], J. Wouter Jukema[2,6], and Bastiaan T. Heijmans[1]

[1] *Molecular Epidemiology, Department of Biomedical Data Sciences, Leiden, the Netherlands.*
[2] *Department of Cardiology, Leiden, the Netherlands.*
[3] *Sequencing Analysis Support Core, Department of Biomedical Data Sciences, Leiden, the Netherlands.*
[4] *Leiden Genome Technology Center, Department of Human Genetics, Leiden, The Netherlands.*
[5] *Department of Medical Biochemistry, Amsterdam UMC, location University of Amsterdam, The Netherlands.*
[6] *Netherlands Heart Institute, Utrecht, The Netherlands.*

*BioRxiv, (2024).*
*Accepted in JACC: Basic to Translational Science*

# Abstract

**Background:** A twice-daily dose of highly purified eicosapentaenoic acid (EPA) reduces the risk of atherosclerotic cardiovascular disease among patients with high triglycerides and either known cardiovascular disease or those at high risk for developing it. However, the process by which EPA exerts its beneficial effects remains poorly understood.

**Objectives:** We show that EPA can induce an anti-inflammatory transcriptional profile in non-activated $CD4^+$ T cells.

**Methods:** Non-activated $CD4^+$ T cells from 8 different donors were exposed to 100μM EPA, oleic acid, palmitic acid, or control. RNA and ATAC-sequencing were performed after 48h of exposure to determine changes in the transcriptomic and epigenetic landscape of the exposed cells as compared to control.

**Results:** We find that EPA-exposed $CD4^+$ T cells downregulate immune response-related genes, such as *HLA-DRA*, *CD69*, and *IL2RA*, while upregulating genes involved in oxidative stress prevention, such as *NQO1*. Furthermore, transcription footprint analysis based on ATAC-sequencing reveals downregulation of GATA3 and PU.1, key transcription factors in $T_H2$ and $T_H9$ differentiation, and upregulation of REV-ERB, an antagonist of $T_H17$ differentiation. By in parallel examining T cell responses to oleic acid, a monounsaturated fatty acid, and palmitic acid, a saturated fatty acid, we find that both the intensity of the transcriptomic response and the involvement of anti-inflammatory pathways is highly specific for EPA.

**Conclusions:** Thus, EPA can induce an anti-inflammatory transcriptomic landscape in $CD4^+$ T cells, a process that may contribute to the unexpectedly strong beneficial effects of EPA on the risk of atherosclerotic cardiovascular disease in clinical trials.


# Highlights

- The mechanism by which EPA reduces the risk of ASCVD in clinical trials remains unclear.
- EPA can induce an anti-inflammatory transcriptomic landscape in non-activated $CD4^+$ T cells *in vitro*.
- T cell reactions to palmitic and oleic acid reveal EPA's unique anti-inflammatory transcriptomic response
- Examining T-cells during IPE interventions may reveal insights into EPA's benefits independent of triglyceride reduction.

# Graphical abstract

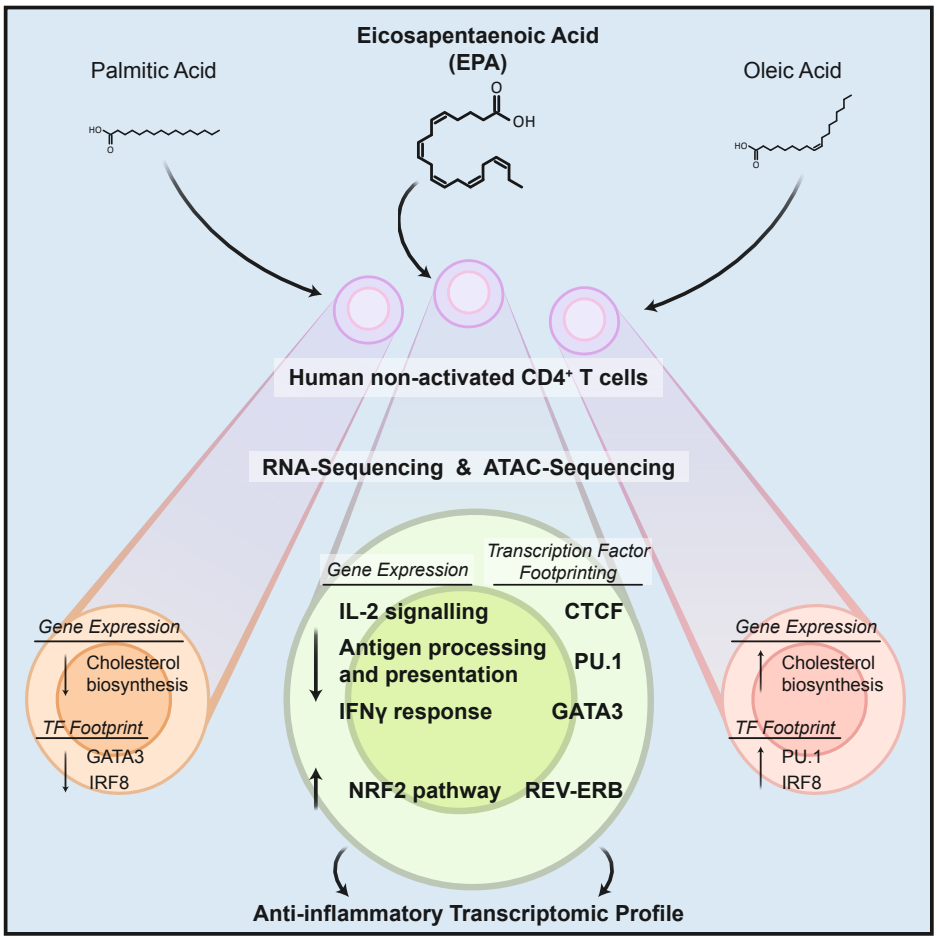

# Introduction

The risk of atherosclerotic cardiovascular disease (ASCVD) persists despite therapies that effectively control blood cholesterol levels including statins and PCSK9 inhibitors[1-3]. This residual risk has been attributed, in part, to elevated triglyceride levels in blood[4]. Nevertheless, most triglyceride influencing therapies, such as fibrates or niacin, have little cardiovascular benefit[5-9]. However, there is one triglyceride lowering drug that was found to strongly reduce ASCVD risk, namely, icosapent ethyl (IPE), which in the body is metabolized to eicosapentaenoic acid (EPA), a polyunsaturated fatty acid. The REDUCE-IT trial showed that patients who received 4g of IPE administered as 2g twice daily was superior to placebo in reducing triglycerides, cardiovascular events, and cardiovascular death among patients with high triglycerides and either known cardiovascular disease or those at high risk for developing it, and who were already on statin therapy with relatively well-controlled low density lipoprotein (LDL) levels[10]. The results of the trial and its interpretation has been much debated in literature[11, 12]. In particular, it remains largely unknown how EPA exerts its beneficial effects, and only limited studies have been carried out in model membranes or by examining whole blood[13-15].

Atherosclerosis is regarded as a lipid-driven immune disease[16]. As such, the majority of immune cells in the atherosclerotic plaque are T cells, of which half are $CD4^+$[17, 18]. Furthermore, $CD4^+$ T cells aggravate atherosclerosis in established mouse models[19, 20]. Therefore, the study of $CD4^+$ T cells is a promising route to further understanding ASCVD and investigating how EPA can influence these cells can indicate a potential mechanism underlying the beneficial effects of EPA on atherosclerosis. Interestingly, EPA was suggested to have anti-inflammatory properties as indicated by a reduction in $CD4^+$ T cell proliferation, decreased differentiation towards T helper 1 ($T_H1$) and T helper 17 ($T_H17$), and increased or no effect on differentiation towards T helper 2 ($T_H2$) and T regulatory ($T_{reg}$) cells[21]. However, these studies were largely carried out in mouse models, or investigated *in vitro* during T cell activation, under polarizing conditions, or by measuring general T cell markers[22-28]. Thus, the effects of EPA on T cells remain incompletely understood and, in particular, it is unknown whether EPA can affect human $CD4^+$ T cells in a non-activated state, as they occur in the circulation and where the primary interaction with EPA takes place.

We aimed to further elucidate the effects of EPA on $CD4^+$ T cells by performing transcriptomic analysis on non-activated exposed cells. Furthermore, we assessed the specificity of the effects of EPA by exposing cells to two other fatty acids of different saturation, oleic acid (OA), a monounsaturated fatty acid, and palmitic acid (PA), a saturated fatty acid. To do so, we performed RNA and ATAC-sequencing on non-activated $CD4^+$ T cells exposed to EPA, OA, PA, or control after 48h exposure. We show that EPA leads to a marked downregulation of many anti-inflammatory genes in non-activated $CD4^+$ T cells as compared to control. The pronounced and specific effects on the transcriptomics landscape contrasted with the relatively modest effects of OA and PA.

# Methods

## Peripheral blood $CD4^+$ T cell isolation and culture conditions

$CD4^+$ T cell isolation and fatty acid exposure model were based on our previously described *in vitro* model with minor changes[29]. To obtain non-activated $CD4^+$ T cells, peripheral blood mononuclear cells (PBMCs) were isolated from 8 different buffy coats of anonymous blood bank donors (Sanquin, Amsterdam, The Netherlands) by Ficoll paque (Apotheek LUMC, 97902861) gradient centrifugation. All donors provided written informed consent in accordance with the protocol of the local institutional review board, the Medical Ethics committee of Sanquin blood supply in accordance with the Declaration of Helsinki. The sex of the cells could not be determined due to the anonymity of the donors. However, RNA sequencing showed that, of 8 donors sequenced, 6 were female and 2 were male, which was accounted for during the statistical analysis by correcting for donor effect. Next, $CD4^+$ T cells were purified from the PBMCs using lyophilized human anti-$CD4^+$ magnetically labeled microbeads (Miltenyi, 130-097-048) scaling the manufacturer's instructions to ⅓ of the recommended volumes. $CD4^+$ T cell purity was assessed on an LSR-II instrument at the Leiden University Medical Center Flow Cytometry Core Facility (https://www.lumc.nl/research/facilities/fcf/) with the BD FACSDiva™ v9.0 software (BD Biosciences). Cells were stained with anti-CD3-PE (BD Biosciences, 345765), anti-CD4-APC (BD Biosciences, 345771), anti-CD8-FITC (BD Biosciences, 555634), and anti-CD14-PEcy7 (BD Biosciences, 560919) and resuspended in 1% paraformaldehyde (Apotheek LUMC, 120810-001) to fix the cells prior to acquisition. Purity was >98% for all donors.

Prior to fatty acid exposure, ~$1*10^8$ isolated cells were cultured overnight to allow the cells to return to a resting state after the stress of the isolation procedure. This was done in T75 flasks (Greiner Bio-One, 658-175) at a density of ~$2.5*10^6$ cells/mL in 5% fetal calf serum (FCS) (Bodinco BDC, 16941) DMEM (Dulbecco's Modified Eagle's Serum (Sigma, 05796), 1% Pen-Strep (Lonza, DE17-602E), 1% GlutaMAX-1 (100x) (Gibco, 35050-038)) medium supplemented with 50 IU/mL IL-2 (Peprotech, 200-02) and incubated at 37°C under 5% $CO_2$. To keep the cells in a non-activated state, no additional stimulus was added. Any $CD4^+$ T cells not used directly after the isolation were kept in DMEM supplemented with 30% FCS, 1% Pen-Strep, 1% GlutaMAX-1, and 20% Dimethyl Sulfoxide (DMSO) (WAK-Chemie Medical GmbH, WAK-DMSO-10) medium at a density of ~$25*10^6$ cells/mL, and stored in liquid nitrogen.

Next, non-activated $CD4^+$ T cells were cultured with either EPA (Cayman, 90110), OA (Sigma, O1383), PA (Cayman, 10006627), or control for 48 hours at 37°C under 5% $CO_2$. The cells were exposed for 48h based off previous findings when establishing our previously described *in vitro* model[29]. To this end, $CD4^+$ T cells from each donor were plated in a 24 wells plate (density of ~$3.5*10^6$ cells/well) in 2mL 5% FCS DMEM for each condition (Fig. 1a). Cells were cultured in medium containing FCS to ensure cell viability during culture and to be more comparable to physiological conditions of the circulation where other lipids are also present. To assess the additional EPA, OA, or PA stimulus to the non-activated $CD4^+$ T cells due to FCS in the culture

medium, an FCS sample was measured via the Shotgun Lipidomics Assistant (SLA) method[30] to estimate the fraction of fatty acids in the sample. The sample was prepped as previously described[31] but with two modifications, a starting volume of 25µL FCS and 600µL MTBE was added instead of 575µL during the first extraction. Free EPA was 0.02µg/mL and EPA as components of larger molecules including cholesterol esters and sphingolipids was 0.13 µg/mL. Free OA was 0.29µg/mL and OA as components of larger molecules including cholesterol esters and sphingolipids was 4.93µg/mL. Free PA was 0.23µg/mL and PA as components of larger molecules including cholesterol esters and sphingolipids was 3.45µg/mL.

PA was dissolved in HPLC grade ethanol (Fisher Scientific, 64-17-5) to a final concentration of 5mg/mL to create a stock solution. The stock solution was vortexed briefly, sonicated in a sonicator (Branson, 2800) for 15 min, and heated for 15 min at 45°C. A small portion of the stock was extracted into a glass HPLC vial (Agilent Technologies, 5182-0714) to a final concentration of 5,000µg/mL. EPA and OA were dissolved from their stock in HPLC grade ethanol to a final concentration of 25,000 and 30,000µg/mL, respectively. The HPLC grade EtOH was then evaporated before the fatty acids were complexed to fatty acid-free (FAF) bovine serum albumin (BSA) (Sigma, A7030) in a 2% FAF BSA DMEM mixture (Dulbecco's Modified Eagle's Serum, 2% FAF BSA, 1% Pen-Strep, 1% GlutaMAX-1 (100x)) to a concentration of 151.25µg/mL for EPA, 141.25µg/mL for OA, and 128.2µg/mL for PA. Complexing fatty acids to BSA mimics physiological conditions as fatty acids are also bound to albumin in the human circulations[32]. Each fatty acid was further diluted to the final concentrations of 100µM (30.25µg/mL for EPA, 28.25µg/mL for OA, and 25.64µg/mL for PA) upon addition to the cells. The concentration tested was kept equal to ensure the cells were exposed the same amount of fatty acid particles and not influenced by concentration differences. Fatty acid stocks were stored under argon gas at -20°C to avoid oxidation.

As a control, HPLC grade EtOH was evaporated in a glass HPLC vial before adding 2% FAF BSA DMEM medium and added to the cells. The amount of 2% FAF BSA DMEM added to the wells was equal for each condition to keep the volumes equivalent. The $CD4^+$ T cells were cultured for 48h at 37°C under 5% $CO_2$. After exposure, the cells were washed and $1*10^5$ cells were used directly for ATAC sequencing preparation. Cells from the same donors for which ATAC sequencing was performed were later thawed from liquid nitrogen and exposed to the fatty acids as described previously. After 48h exposure, the cells were washed and $3*10^6$ cells were flash frozen in liquid nitrogen and stored at -80°C for RNA isolations. Cell viability and diameter were measured by Via1-Cassette™ (Chemometec, 941-0012) on a NucleoCounter® NC-200™ (Chemometec, 900-0200) and found to be > 95% and on average 9µm for each condition.

## RNA isolation

To isolate total RNA for RNA sequencing and RT-qPCR, RNA was extracted from the cell samples using the Quick-RNA Microprep Kit (Zymo, R1050) according to manufacturer's instructions. The RNA was quantified using a Qubit® 2.0 Fluorometer (Q32866) with the Qubit® RNA BR Assay Kit (Thermofisher, Q10211) according to manufacturer's instructions. The RNA was placed over a second Zymo-Spin IC Column, washed, and a second DNase treatment performed to

remove any residual DNA contamination from the samples. RNA integrity (RIN) values of the samples were on average 7.8 SE 0.1 as determined using an Agilent 2100 Bioanalyzer Instrument (G2939BA) with the Agilent RNA 6000 Nano Reagents (Agilent, 5067-1511). RNA was divided into two samples and stored at -80°C, 1µg for RNA sequencing and the rest for cDNA synthesis and RT-qPCR measurements.

## Real time-quantitative PCR

To measure the expression of *CPT1A* in all the cell samples, cDNA was synthesized with 200ng of the stored RNA using the Transcriptor First Strand cDNA Synthesis Kit (Roche, 04897030001) according to the manufacturer's instructions. Quantitative real time PCR's for *CPT1A* (Thermofisher, Hs00912671_m1, 4331182) were performed using the TaqMan™ Fast Advanced Master Mix (Thermofisher, 4444557) with 10ng cDNA per reaction on a QuantStudio 6 Real-Time PCR system (Applied Biosystems). All RT-qPCR reactions were performed in triplicate and outliers were removed if the Ct value measured differed more than 0.5% from the mean. Relative gene expression levels (-ΔCt) were calculated using the average of Ct values of *RPL13A* (Thermofisher, Hs03043887_gH, 4448892) and *SDHA* (Thermofisher, Hs00188166_m1, 4453320) as internal controls[33]. The fold change was determined using the $2^{-\Delta\Delta Ct}$ method, using the control as the reference. All statistical analyses were performed in R. Data are expressed as mean of the relative fold change and standard error. The reported P values were determined by applying a paired two-tailed student's T test. P values < 0.05 were considered to be statistically significant.

## RNA sequencing analysis

RNA sequencing (RNA-seq) was performed to determine the differences in the transcriptome of control versus fatty acid exposed non-activated $CD4^+$ T cells across time. The RNA from each of the samples was sent for sequencing (Macrogen, Amsterdam, NL). RNA-sequencing libraries were prepared from 200ng RNA using the Illumina Truseq stranded mRNA library prep (Illumina, 20020594) with a poly A selection. Both whole-transcriptome amplification and sequencing library preparations were performed in two 96-well plates with 26 samples in one plate and 6 in another. Quality control steps were included to determine total RNA quality and quantity, the optimal number of PCR preamplification cycles, and fragment size selection. No samples were eliminated from further downstream steps. Barcoded libraries were divided across two plates with 26 samples in one and 6 in the other and sequenced separately. Barcoded libraries were sequenced to a read depth of 20 million reads using the Novaseq 6000 (Illumina) to generate 100 base pair paired-end reads.

FastQ files are analyzed using the RNAseq pipeline (v5.0.0) from BioWDL (https://zenodo.org/record/5109461), developed by SASC (LUMC). The pipeline performed preprocessing on the FastQ files (including quality control, quality trimming, and adapter clipping), read mapping, and expression quantification. *FastQC* (v0.11.9) is used to check raw reads and *Cutadapt* (v2.10) to perform adapter clipping. Reads are mapped to a reference genome (Ensembl v105) using *STAR aligner* (v2.7.5a), and with *HTSeq Count* (v0.12.4) the number of assigned reads to genes per sample is determined.

Based on Ensembl gene biotype annotation, we included only protein coding genes for further downstream analysis (19,991 genes in total). We used the Bioconductor package *DESeq2*[34] (v1.40.2) to test whether EPA, OA, or PA had an effect on gene expression as compared to the control. *DESeq2* fits a generalized linear model (GLM) assuming the negative binomial distribution for the counts. The model expresses the logarithm of the average of the counts in terms of one or more predictors. In this case, we used three models that had one of the fatty acids, subject identifier, and batch as predictors each. By including the subject identifier and batch in the models, we account for the dependence between measurements within the same subject and between different batches of sequencing[34]. Lowly expressed genes, i.e. that did not have at least a count of 1 in half of the samples per fatty acid and control, were removed, resulting in 12,938 genes for EPA, 12,949 genes for OA, and 12,971 genes for PA. The Benjamini-Hochberg procedure was used to correct for multiple testing at a false discovery rate (FDR) of 5%.

Differentially expressed genes per fatty acid were divided into upregulated or downregulated based on the log2 fold change values. 10 human pathway databases (BioPlanet 2019, WikiPathways 2019 Human, KEGG 2019 Human, Elsevier Pathway Collection, BioCarta 2015, Reactome 2016, HumanCyc 2016, NCI-Nature 2016, Panther 2016 and MSigDB Hallmark 2020) were queried using gene symbols, with 904 of 1170 queried genes for EPA, 51 of 60 queried genes for OA, and 26 of 33 queried genes for PA, present in at least 1 database. The identified clusters were then mapped for pathway enrichment using *clusterProfiler*[35] (v4.8.3) with the background set to the 12,938 expressed genes for EPA, 12,949 expressed genes for OA, and 12,971 expressed genes for PA as determined above. Multiple testing correction using the Benjamini-Hochberg method at 5% FDR was performed over the combined results from the 10 databases. Pathways that included highly similar gene sets were grouped (Jaccard index > 0.7) and only the most significantly enriched pathway per group was retained.

## ATAC sequencing analysis

Post-exposure, the $1*10^5$ cells were taken off for ATAC sequencing and placed into DNA LoBind 1.5mL tubes (Eppendorf, 2231000945). The cells were washed 3x in ice cold buffered natrium chloride (PBS; pH 7.4; Fresen, 15360679). The samples were then handed off to the Leiden Genome Technology Center for library generation. The ATAC-sequencing libraries were generated using the Omni-ATAC protocol[36]. Briefly, the nuclei were isolated by lysing the cells in ATAC-Resuspension Buffer (RSB) (0.1% NP40 (Thermofisher, 85124), 0.1% Tween-20 (Thermofisher, 28320), and 0.01% digitonin (Promega, G9441)) for 3 min on ice. After washing the nuclei with 1mL wash buffer (RSB and 0.1% Tween) the nuclei were centrifuged for 10min at 4°C. After removing the supernatant, carefully avoiding the pelleted nuclei, the nuclei were resuspended in PBS. The nuclei were counted and normalized to 25,000 cells using the TC20 cell counter (BioRad, 1450102). The nuclei were combined with 25µL 2x TD buffer (TrisHCl pH 7.5 (Thermofisher, 15567027), NaCl (Thermofisher, A57006) and MgCl2 (Thermofisher, AM9530G)), 2µL Tn5 enzyme (Tn5 enzyme (Illumina, 15027865) and TD Tagment DNA Buffer (Illumina, 15027866)), 0.5µL 1% digitonin, 0.5µL 10% Tween-20 up to a volume of 50µL. The reaction was incubated at 37°C for 30min and then purified using AMPure Beads (Beckman Coulter, A63881) with a ratio of 1.8x and

eluted in 10µL of EB (10mM Tris-HCl). The PCR was done using 2x Kapa HiFi Master mix (Roche, 09420398001) with the barcoded primers described in the Omni-ATAC protocol. After the PCR, the products were dual size selected using AMpure beads, first using 0.4x, followed directly by 1.2x. The ATAC-sequencing libraries were checked on the Femto Pulse (Agilent, M5330AA) and pooled equimolar for sequencing. No samples were eliminated from further downstream steps.

Barcoded libraries were sent for sequencing (Macrogen, Amsterdam, NL). An additional round of quality control was performed and the samples were then pooled and divided across one lane. Barcoded libraries were sequenced to a read depth of 30 million 150 base pair paired-end reads using the Novaseq 6000 (Illumina).

FastQ files were analyzed using the ChIP-seq pipeline from BioWDL (https://github.com/biowdl/ChIP-seq), developed by SASC (LUMC). The pipeline performed preprocessing on the FastQ files (including quality control, quality trimming, and adapter clipping), read mapping, and peak calling. *FastQC* (v0.11.9) is used to check raw reads and *Cutadapt* (v2.10) to perform adapter clipping. Reads are mapped to a reference genome (Encode GRCh38) using *BWA aligner* (v0.7.17), and *MACS2* (v2.1.2) was used to perform the peakcalling. These peak files were then processed using R (v4.3.0). Using *DiffBind* (v3.10.0), reads in the BAM files were counted for each peak. Next, the read counts per peak for each sample were merged to create one table containing all peaks and read counts of all the samples combined. *De novo* motif analysis was then performed using HOMER[37].



### Data availability

The data supporting the findings of this study are available within the article and its Supplementary information files. All other data including the raw files are available at the Gene Expression Omnibus repository, accession GEO (main combined submission: GSE254749, RNA sequencing submission: GSE254695, and ATAC sequencing submission: GSE254468).

## Results

### Transcriptomic analysis of EPA exposed non-activated CD4+ T cells

Non-activated CD4+ T cells from 8 different donors were each exposed to 100µM EPA, OA, PA, or control for 48h (Fig. 1a). Exposure did not affect cell viability or diameter (Supp. Fig. 1a and b). To confirm a response by the cells due to the fatty acid exposure, the expression of *CPT1A*, the rate limiting enzyme in β-fatty acid oxidation, was measured. *CPT1A* expression increased as compared to control (EPA: 12.4-fold, SE 1.9 ($p < 0.001$); OA: 19.5-fold, SE 3.0 ($p < 0.001$); PA: 11.3-fold, SE 2.2 ($p < 0.003$); Fig. 1b). This signifies a consistent response to EPA, OA, and PA exposure.

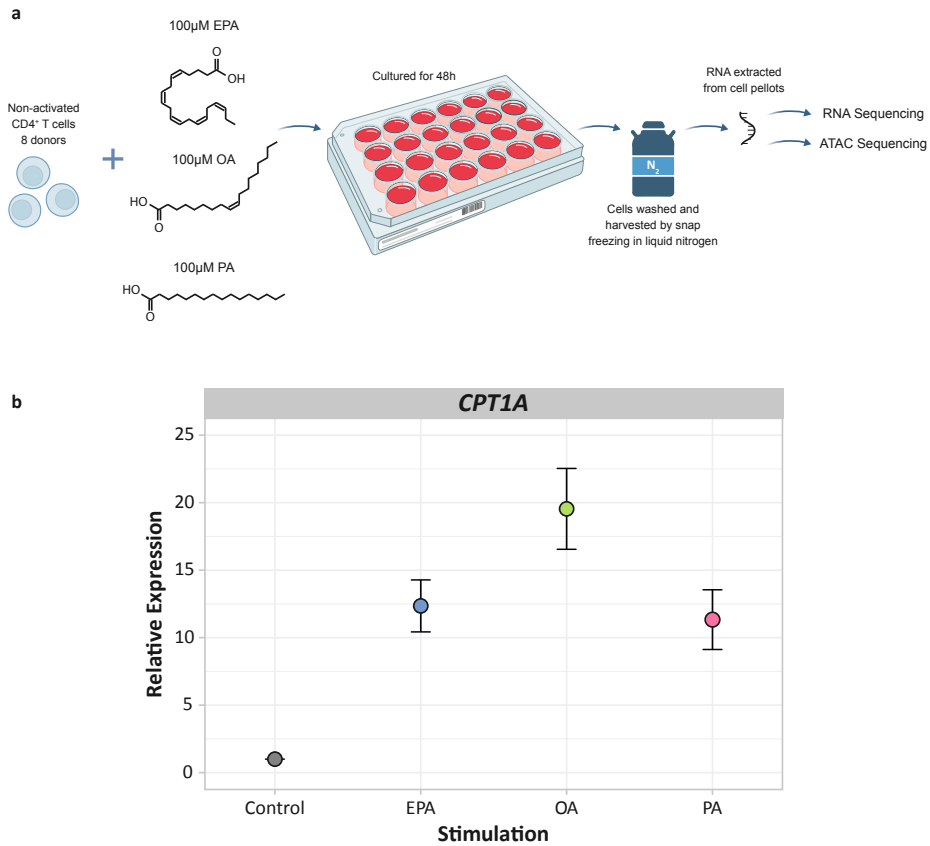


**Fig. 1 | Experimental set up and *in vitro* model verification. (a)** Experimental set up for RNA and ATAC sequencing of EPA, OA, and PA exposed non-activated CD4⁺ T cells, n = 8. **(b)** Dot plot showing the relative expression of *CPT1A* after 48h of fatty acid exposure as a confirmation of the *in vitro* model by RT-qPCR. Values are colored by fatty acid. On average *CPT1A* was upregulated 12.4 SE 1.9 fold for EPA ($p < 0.001$), 19.5 SE 3.0 fold for OA ($p < 0.001$), and 11.3 SE 2.2 fold for PA ($p < 0.003$), n = 8. Abbreviations, EPA = eicosapentaenoic acid, h = hours, OA = oleic acid, PA = palmitic acid.

Next, we studied the transcriptomic response of CD4⁺ T cells to EPA, OA, and PA as compared to control using RNA-seq. The transcriptional response was compared to the control condition for each fatty acid. The number of differentially expressed genes (DEGs) and effect sizes were markedly larger for EPA, than for OA and PA (Fig. 2a) and there was limited overlap between the DEGs of each fatty acid (Fig. 2b). EPA induced 1170 DEGs ($P_{FDR} < 0.05$), 723 of which were downregulated and 447 of which were upregulated (Supp. Table 1a and b). In contrast, OA induced 60 DEGs ($P_{FDR} < 0.05$; 13 downregulated and 47 upregulated; Supp. Table 1c and d). PA induced found 33 DEGs ($P_{FDR} < 0.05$; 15 downregulated and 18 upregulated; Supp. Table 1e and f). Despite the high specificity of the transcriptional response of each fatty acid, 4 genes were upregulated upon exposure of all three fatty acids. These genes were involved in β-fatty acid oxidation (*CPT1A*, *SLC25A20*, *ACADVL*, and *ACAA2*) in line with a generic cellular response to fatty acid exposure regardless of the fatty acid type (Supp. Table 1g).

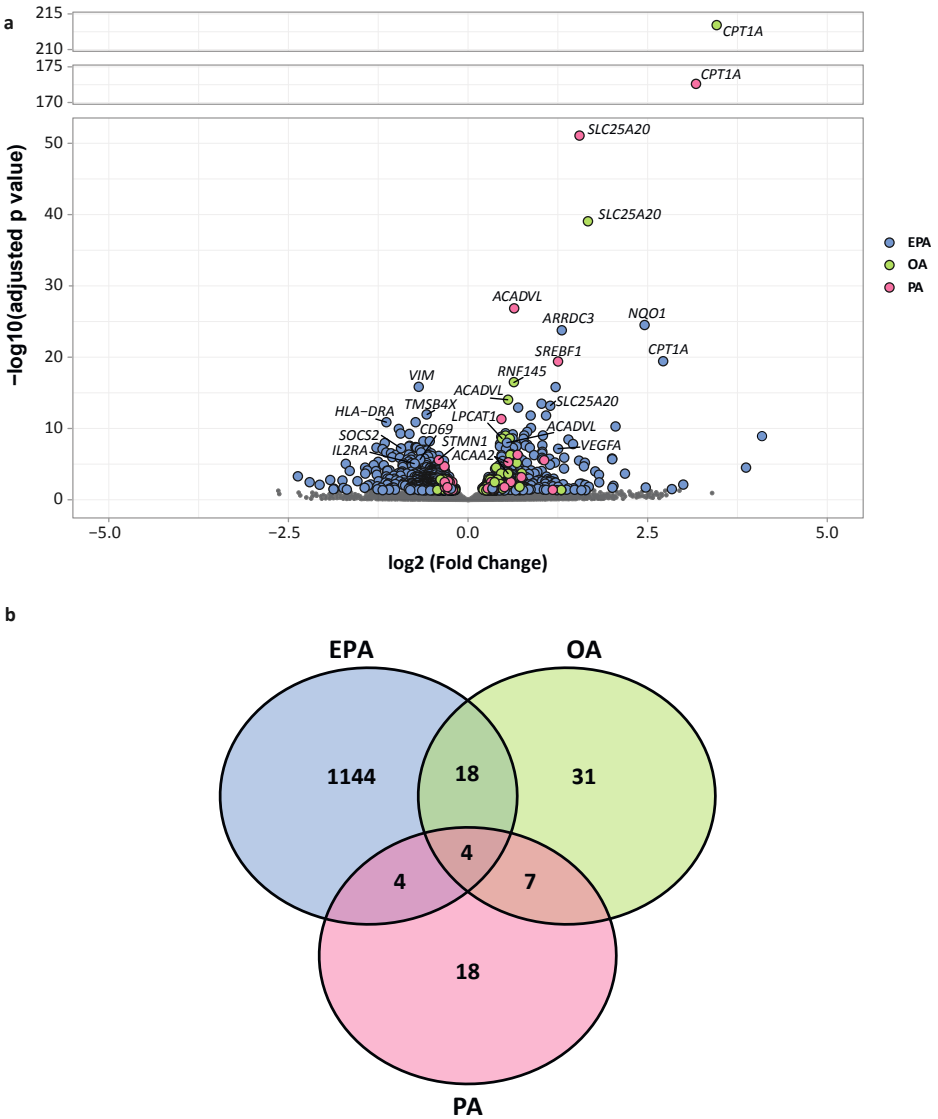


**Fig. 2 | EPA, OA, and PA exposure in non-activated CD4⁺ T cells induces changes in transcriptomics. (a)** Volcano plot showing the gene expression of non-activated CD4⁺ T cells exposed to either EPA, OA, or PA. All 19,991 protein coding genes are shown for each fatty acid. DEGs are colored by fatty acid and denoted by a larger size. Non-significant genes are shown in grey and denoted by a smaller size. Log2 fold change is used to show the direction of gene expression. **(b)** Venn diagram showing the unique response of non-activated CD4⁺ T cells to each fatty acid. Values are colored by fatty acid. There are 6 DEGs overlapping between all three fatty acids, 18 DEGs overlapping between EPA and OA, 4 DEGs overlapping between EPA and PA, and 7 DEGs overlapping between OA and PA. Abbreviations, EPA = eicosapentaenoic acid, OA = oleic acid, PA = palmitic acid.

We focused on the marked transcriptomic response of $CD4^+$ T cells to EPA. Firstly, we analyzed the 723 downregulated genes in EPA exposed non-activated $CD4^+$ T cells. The top three DEGs were *VIM* (vimentin), *TMSB4X* (thymosin beta 4 X-linked) and *HLA-DRA* (major histocompatibility complex, class II, DR alpha). *VIM* and *TMSB4X* both encode structures involved in the makeup of the cytoskeleton. HLA-DRA plays a central role in the immune response by presenting peptides to T cells. Remarkably, many other immune response genes were also downregulated, including *SOCS2* (suppressor of cytokine signaling 2), *CD69* (CD69 molecule), and *IL2RA* (interleukin 2 receptor subunit alpha). SOCS2 is a negative regulator of cytokine receptor signaling, particularly of IGF1R, an Insulin-Like Growth Factor whose expression is associated with the development of $T_H17$ over $T_{reg}$ subsets. CD69 plays an integral part in T cell activation, and IL2RA is an important regulator of T cell differentiation. A strong downregulation of immune-related processes was confirmed by a formal analysis of enriched biological processes. In particular, interleukin (IL)-2 signaling pathway ($P_{FDR} < 0.001$; 110 DEGs), antigen processing and presentation ($P_{FDR} < 0.001$; 27 DEGs), and interferon gamma response ($P_{FDR} < 0.001$; 47 DEGs) were enriched (Fig. 3a; Supp. Table 1h). This indicates that EPA reduces immune related gene expression in non-activated $CD4^+$ T cells.

Secondly, we analyzed the 447 upregulated genes in EPA exposed non-activated $CD4^+$ T cells. The top three DEGs were *NQO1* (NAD(P)H quinone dehydrogenase 1), *ARRDC3* (arrestin domain containing 3) and *CPT1A*. NQO1 is involved in protecting cells against oxidative stress, which can be caused by lipid peroxidation and *ARRDC3* encodes a regulator of G protein-mediated signaling. Another gene of interest that was upregulated was *VEGFA* (vascular endothelial growth factor A). The enzyme encoded by this gene is a proangiogenic molecule known to be involved in creating immunosuppressive environments. This immunosuppressive profile was further supported by a formal analysis of enriched biological processes, which showed upregulation of the NRF2 pathway ($P_{FDR} < 0.001$; 20 DEGs; Fig. 3b; Supp. Table 1i). This pathway is the most important pathway for protecting cells against oxidative stress and has been shown to be involved in anti-inflammatory responses. Overall, these results suggests that EPA exposure can alter gene expression in non-activated T cells towards an anti-inflammatory profile by decreasing immune response related genes and increasing protective genes such as those in the NRF2 pathway.

Next, we investigated whether specific transcription factors may underlie the differential gene expression. To do this, we examined the enrichment of transcription factor binding motifs in loci that were more closed (down) versus more open (up) as determined by ATAC-sequencing. The top EPA downregulated motifs included CTCF, GATA3, RUNX1, and PU.1 (Fig. 3c; Supp. Table 1j). CTCF is a master regulator of chromatin looping and moreover, involved in effector cell differentiation[38, 39]. GATA3 and PU.1 are the key transcription factors for the development of $T_H2$ and $T_H9$ cells, respectively[40, 41]. RUNX1 is necessary for T cell maturation, knock outs of this transcription factor results in phenotypically and functionally immature T cells[42]. We next examined the enrichment of transcription factor binding motifs in upregulated versus downregulated genes. EPA upregulated motifs included, REV-ERB, TCF7, and FOXA1 (Fig. 3d; Supp. Table 1k). REV-ERB is an antagonist of RORγt, the key transcription factor for the development of $T_H17$ cells[43]. TCF7 plays a role in the regulation of autoinflammatory T cell responses[44]. FOXA1

is involved in giving $T_{reg}$ cells their suppressive properties[45]. These results further suggest that non-activated CD4$^+$ T cells may decrease their ability to induce an immune response or effector T cell profile after EPA exposure.

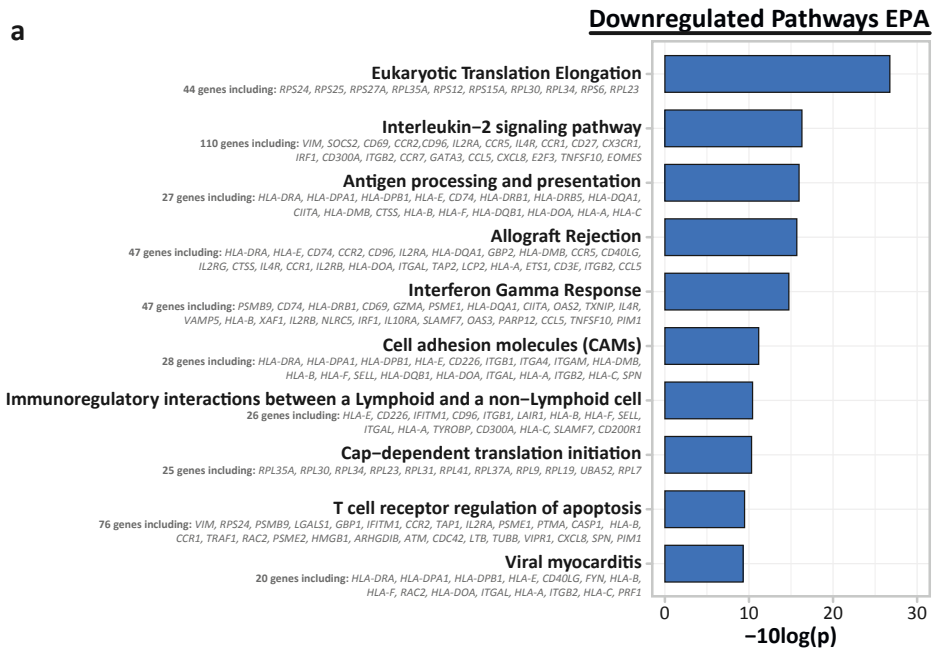


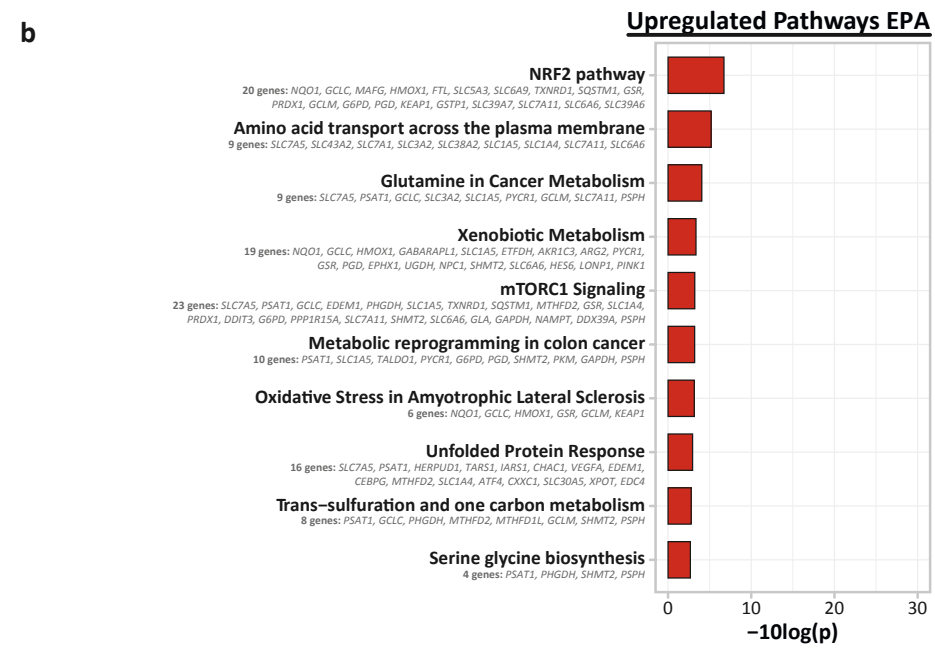

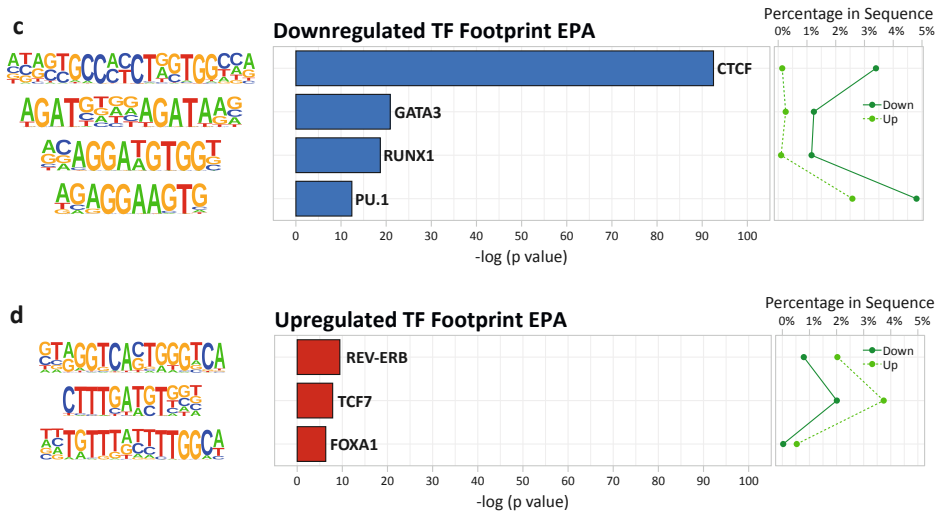


**Fig. 3 | Up- and downregulated pathways and transcription factors in EPA-exposed non-activated CD4⁺ T cells. (a)** Pathway enrichment analysis of all downregulated EPA DEGs generated using *clusterProfiler* using 10 human pathway databases. Top 10 enrichments are shown. **(b)** Pathway enrichment analysis of all upregulated EPA DEGs generated using *clusterProfiler* using 10 human pathway databases. Top 10 enrichments are shown. **(c)** Known motif analysis on promotors of down versus upregulated EPA ATAC peaks. Enrichment of transcription factor binding motifs was performed using HOMER. 4 motifs are shown with supplementing information on p-value, percentage of genes in upregulated gene set and percentage of genes in downregulated gene set, transcription factor name, -log(p-value), and percentage in sequence. **(d)** Known motif analysis on promotors of up versus downregulated EPA ATAC peaks. Enrichment of transcription factor binding motifs was performed using HOMER. 4 motifs are shown with supplementing information on p-value, percentage of genes in upregulated gene set and percentage of genes in downregulated gene set, transcription factor name, -log(p-value), and percentage in sequence. Abbreviations, EPA = eicosapentaenoic acid, TF = transcription factor.

## Transcriptomic analysis of OA and PA exposed non-activated CD4⁺ T cells

Non-activated CD4⁺ T cells were also exposed to either OA or PA and differential gene expression was measured. In line with our previous experiments, we found that OA exposure lead to the downregulation of endogenous peptide antigen presentation (*HSPA5* and *PDIA3*; $P_{FDR} < 0.001$; 2 DEGs), electron transport chain and oxidative phosphorylation activity (*NDUFA12*, *NDUFB4*, and *ATP5F1C*; $P_{FDR} < 0.001$; 3 DEGs) and upregulation of cholesterol biosynthesis (*HMGCR*, *HMGCS1* and *DHCR24*; $P_{FDR} < 0.001$; 4 DEGs; Supp. Fig. 2a and b; Supp. Table 1l and m) related genes. Exposure to PA induced an opposite response, with the downregulation of cholesterol biosynthesis pathway (*HMGCR* and *SQLE*; $P_{FDR} < 0.05$; 2 DEGs), and upregulated beta fatty acid oxidation (*CPT1A*, *SLC25A20*, and *ACADVL*; $P_{FDR} < 0.001$; 3 DEGs; Supp. Fig. 2c and d; Supp. Table 1n and o) related genes. Thus, the changes in the transcriptome of OA and PA exposed cells seem to have a greater effect on genes involved in cellular metabolism, particularly cholesterol metabolism, as compared to EPA.

The transcriptional responses observed were in line with the results of ATAC-sequencing based transcription factor footprint analysis. For OA only three motifs were downregulated including RAR:RXR, a motif known to play a part in the development of $T_{reg}$ over $T_H17$ cells (Supp. Fig. 3a;

Supp. Table 1p). OA upregulated motifs included PU.1, as was found previously[29] as well as IRF8, which is also involved in $T_H9$ differentiation (Supp. Fig. 3b; Supp. Table 1q). PA downregulated motifs included IRF8 and GATA3 (Supp. Fig. 3c; Supp. Table 1r) and upregulated motifs included REV-ERB (Supp. Fig. 3d; Supp. Table 1s). OA and PA showed reversed effects on cholesterol metabolism processes which were mirrored in opposite associations with transcription factor binding motifs, indicating fatty-acid specific responses in non-activated $CD4^+$ T cells.

# Discussion

IPE, the highly purified form of EPA, has been associated with reduced triglycerides, cardiovascular events, and cardiovascular death in individuals with relatively well controlled LDL levels, even when corrected for placebo response in the mineral oil control group, LDL, and C-reactive protein (CRP) in the REDUCE-IT trial[10, 46-49]. The trials outcomes and interpretation have been widely debated and the mechanisms by which EPA exerts its beneficial effects remains incompletely understood[11, 12]. We show that EPA exposure can already produce distinct changes in T cells prior to activation by decreasing the expression of immune response genes and increasing the expression of genes involved in oxidative stress protection. This is further supported by changes in transcription factor binding sites in our ATAC-sequencing motif analysis, indicating a change in the epigenetic landscape of EPA exposed T cells. Furthermore, we show that EPA induces a unique response in non-activated $CD4^+$ T cells as two other fatty acids of varying degrees of saturation, OA and PA, generated a smaller yet distinct effect on gene expression profiles in T cells as compared to control. Our findings imply that different fatty acids in the circulation can induce diverse effects on T cell transcriptomics, and that specifically EPA exposure may poise T cells to have clearer anti-inflammatory responses. These results underscore a potential mechanism by which EPA may mitigate ASCVD risk, suggesting its anti-inflammatory impact on T cells as a contributing factor. This is particularly noteworthy as T cells comprise over half of the immune cell population within atherosclerotic plaques[17, 18].

Our results show that EPA exposure, but not OA nor PA, leads to a strong downregulation of immune response related genes. Particularly, genes involved in antigen processing and presentation were downregulated in EPA exposed cells, denoted by, amongst others, the decreased expression of 14 different HLA genes. This gene group is crucial in inducing immune responses[50] and has also been found to be associated with T cell activation and effector memory phenotype in $CD4^+$ T cells[51]. In addition, genes involved in IL-2 signaling were also downregulated, which is required for T cell activation[52]. Downregulation of genes in these pathways suggests that EPA exposed T cells may have a reduced ability to initiate an immune response, a key component of inflammatory responses in atherosclerotic plaques[53]. This result can support the finding that higher plasma EPA levels are associated with lower CVD risk in humans[54]. Furthermore, genes involved in pro-inflammatory pathways, such as interferon gamma response were downregulated in EPA exposed cells. IFNγ is primarily produced by pro-inflammatory T cell subset, $T_H1$ cells, which have also been found to decrease upon EPA exposure[27, 55-57]. Moreover, the key transcription

factors in $T_H2$ and $T_H9$ differentiation, GATA3 and PU.1, were also found to be decreased in our motif analysis. While $T_H2$ cells have inconclusive effects on ASCVD, $T_H9$ cells have been shown to aggravate it[58-60]. Thus, EPA exposure decreased genes involved in immune response and pro-inflammatory pathways as well as suggests a reduced ability for key T cell differentiation transcription factors to bind.

In further support of EPA's anti-inflammatory properties on non-activated $CD4^+$ T cells, we found that genes involved in the NRF2 pathway were upregulated upon EPA exposure. This pathway mainly functions in preventing oxidative stress in cells by activating genes involved in detoxification and removal of reactive oxygen species[61]. However, the NRF2 pathway has also been shown to aid in the anti-inflammatory responses of macrophages[62] and has been suggested as a beneficial pleiotropic effect of statins[63], as oxidative stress has been found to be a risk factor for ASCVD[64]. We also found an increased footprint for the transcription factors REV-ERB, TCF7, and FOXA1. These transcription factors are each involved in regulating T cell responses and generating a more anti-inflammatory T cell profile[43-45]. Overall, these data indicate that non-activated $CD4^+$ T cells can already acquire an anti-inflammatory transcriptomic profile, which may play a role in the anti-inflammatory properties observed of EPA in clinical trials.

EPA has a distinct effect on $CD4^+$ T cells. This is observed by our analysis of the effects of OA and PA on non-activated $CD4^+$ T cells. The number of DEGs and effect sizes were smaller upon OA and PA exposure and distinctly different. Interestingly, OA and PA each had opposed effects on cholesterol biosynthesis related genes, with OA upregulating and PA downregulating genes in this pathway. Upregulation of cholesterol biosynthesis has been related to the development of $T_H17$ cells by controlling RORγt activity, the key transcription factor in $T_H17$ differentiation[65, 66]. This observation can be further supported by OA downregulating the RAR:RXR motif, which is involved in generating $T_{reg}$ cells over $T_H17$ and PA upregulating REV-ERB[43, 67]. The results of OA exposure also show the robustness of our approach as our findings here match what was found previously by our group[29]. These data suggest that our model is robust and each fatty acid induces its own unique response in non-activated $CD4^+$ T cells.

# Conclusion

In conclusion, our data points to the fact that EPA produces a strong and specific anti-inflammatory transcriptional profile in non-activated $CD4^+$ T cells comprised of both the downregulation of immune related genes and the upregulation of antioxidant genes. This profile is supported by transcription factor motif analysis and by the analysis of two other fatty acids of varying degrees of saturation. Our results contribute to the debate of how EPA exerts beneficial effects in human ASCVD. Our study gives an indication that the beneficial effects observed of EPA, as asserted in clinical trials, can already start in the circulation by inducing an anti-inflammatory transcriptional profile in non-activated T cells with potentially anti-atherosclerotic properties.

# Limitations of the study

We show that EPA exposure has beneficial anti-inflammatory effects on non-activated $CD4^+$ T cells. This is relevant because T cells are largely non-activated in the circulation and it is in the circulation where T cells will encounter EPA when individuals are treated with IPE to reduce ASCVD risk. Nevertheless, our results are in line with experiments on activated T cells, which showed that EPA exposure decreased proliferation[22-26], decreased $T_H1$ and $T_H17$ populations[27, 28], and had no effect on or increased $T_H2$ and $T_{reg}$ populations[26-28]. Therefore, the encounter with EPA in a non-activated state may induce transcriptomic changes that influence the functional changes post-activation. Furthermore, our use of non-activated $CD4^+$ T cells with no additional selection towards naïve, effector, memory, or specific T helper subsets, as well as in culture medium containing other lipids more closely represents the diversity of T cells and environment of the circulation in which EPA exposure takes place. Additionally, we utilized OA and PA, two fatty acids of varying degrees of saturation to establish the distinct effects of EPA. Nevertheless, this does not rule out that other fatty acids may have marked effects on non-activated $CD4^+$ T cells as well[21]. A final limitation of our study is that we have employed an *in vitro* model and the effects of EPA on T cells *in vivo* should be studied in the context of trials of IPE. However, in mouse models, EPA supplementation has also been shown to reduce cholesterol levels[68], whereas, in humans, the effects of EPA on ASCVD risk were independent of LDL lowering[47]. Therefore, using a validated *in vitro* model provides valuable insights to study the effects of EPA on human $CD4^+$ T cells.



# Translational perspectives

We report that EPA induces an anti-inflammatory transcriptomic profile in non-activated $CD4^+$ T cells. This observation is important to better understand the mechanism through which EPA reduces cardiovascular disease risk in studies such as the REDUCE-IT trial. The REDUCE-IT trial showed that intervention with IPE, which the body metabolizes to EPA, reduces the risk of cardiovascular events and death in patients with high triglycerides. The findings of this trial have sparked considerable debate in the literature as the results appeared to occur irrespective of the attained triglyceride level after one year[10-12]. Testing T cells from individuals undergoing IPE interventions can provide additional insights into how EPA exerts its beneficial effects independent of triglyceride reduction.

**Acknowledgements**
The authors' work is supported by the Dutch CardioVascular Alliance (The Dutch Heart Foundation, Dutch Federation of University Medical Centers, the Netherlands Organization for Health Research and Development, and the Royal Netherlands Academy of Sciences) for the GENIUSII project Generating the Best Evidence-Based Pharmaceutical Targets for Atherosclerosis (CVON2017-20).

**Author contributions**
B.T.H and J.W.J conceived the project. N.A.R. designed and conducted the experiments, analyzed the results, and drafted the manuscript. K.F.D. designed the analysis model and analyzed the RNA sequencing data. J.M. designed and performed *in vitro* model and prepped samples for ATAC sequencing. S. A. designed and performed *in vitro* model and prepped samples for RNA sequencing. T.K. aligned the RNA and ATAC sequencing data. Y.A. performed the ATAC sequencing library preparation. M.A.H. performed and analyzed the transcription factor footprint analysis. All authors contributed to the writing of the manuscript.

**Competing interests**
The authors declare no competing interests.

# References


1 Lawler, P. R. *et al.* Targeting cardiovascular inflammation: next steps in clinical translation. *Eur. Heart J.* **42**, 113-131, (2021).

2 Sabatine, M. S. *et al.* Evolocumab and clinical outcomes in patients with cardiovascular disease. *N. Engl. J. Med.* **376**, 1713-1722, (2017).

3 Schade, D. S. & Eaton, R. P. Residual cardiovascular risk—is inflammation the primary cause? *World J. Cardiovasc. Dis.* **08**, 59-69, (2018).

4 Lawler, P. R. *et al.* Real-world risk of cardiovascular outcomes associated with hypertriglyceridaemia among individuals with atherosclerotic cardiovascular disease and potential eligibility for emerging therapies. *Eur. Heart J.* **41**, 86-94, (2020).

5 The ACCORD Study Group. Effects of intensive blood-pressure control in type 2 diabetes mellitus. *N. Engl. J. Med.* **362**, 1575-1585, (2010).

6 Keech, A. *et al.* Effects of long-term fenofibrate therapy on cardiovascular events in 9795 people with type 2 diabetes mellitus (the FIELD study): randomised controlled trial. *Lancet* **366**, 1849-1861, (2005).

7 Das Pradhan, A. *et al.* Triglyceride lowering with pemafibrate to reduce cardiovascular risk. *N. Engl. J. Med.* **387**, 1923-1934, (2022).

8 The AIM-HIGH Investigators. Niacin in patients with low HDL cholesterol levels receiving intensive statin therapy. *N. Engl. J. Med.* **365**, 2255-2267, (2011).

9 The HPS2-THRIVE Collaborative Group *et al.* Effects of extended-release niacin with laropiprant in high-risk patients. *N. Engl. J. Med.* **371**, 203-212, (2014).

10 Bhatt, D. L. *et al.* Cardiovascular risk reduction with icosapent ethyl for hypertriglyceridemia. *N. Engl. J. Med.* **380**, 11-22, (2019).

11 Kastelein, J. J. P. & Stroes, E. S. G. FISHing for the miracle of eicosapentaenoic acid. *N. Engl. J. Med.* **380**, 89-90, (2019).

12 Steg, P. G. & Bhatt, D. L. The reduction in cardiovascular risk in REDUCE-IT is due to eicosapentaenoic acid in icosapent ethyl. *Eur. Heart J.* **42**, 4865-4866, (2021).

13 Mason, R. P., Jacob, R. F., Shrivastava, S., Sherratt, S. C. R. & Chattopadhyay, A. Eicosapentaenoic acid reduces membrane fluidity, inhibits cholesterol domain formation, and normalizes bilayer width in atherosclerotic-like model membranes. *Biochim. Biophys. Acta* **1858**, 3131-3140, (2016).

14 Tsunoda, F. *et al.* Effects of oral eicosapentaenoic acid versus docosahexaenoic acid on human peripheral blood mononuclear cell gene expression. *Atherosclerosis* **241**, 400-408, (2015).

15 Vors, C. *et al.* Inflammatory gene expression in whole blood cells after EPA vs. DHA supplementation: results from the ComparED study. *Atherosclerosis* **257**, 116-122, (2017).

16 Wolf, D. & Ley, K. Immunity and inflammation in atherosclerosis. *Circ. Res.* **124**, 315-327, (2019).

17 Fernandez, D. M. *et al.* Single-cell immune landscape of human atherosclerotic plaques. *Nat. Med.* **25**, 1576-1588, (2019).

18 Depuydt, M. A. *et al.* Microanatomy of the human atherosclerotic plaque by single-cell transcriptomics. *Circ. Res.* **127**, 1437-1455, (2020).

19 Zhou, X., Robertson, A. K., Hjerpe, C. & Hansson, G. K. Adoptive transfer of CD4+ T cells reactive to modified low-density lipoprotein aggravates atherosclerosis. *Arterioscler. Thromb. Vasc. Biol.* **26**, 864-870, (2006).

20 Zhou, X., Nicoletti, A., Elhage, R. & Hansson, G. K. Transfer of CD4+ T cells aggravates atherosclerosis in immunodeficient apolipoprotein E knockout mice. *Circulation* **102**, 2919-2922, (2000).

21 Reilly, N. A., Lutgens, E., Kuiper, J., Heijmans, B. T. & Wouter Jukema, J. Effects of fatty acids on T cell function: role in atherosclerosis. *Nat. Rev. Cardiol.* **18**, 824–837, (2021).

22 Fan, Y. Y. *et al.* Remodelling of primary human CD4+ T cell plasma membrane order by n-3 PUFA. *Br. J. Nutr.* **119**, 163-175, (2018).

23 Gorjão, R., Cury-Boaventura, M. F., de Lima, T. M. & Curi, R. Regulation of human lymphocyte proliferation by fatty acids. *Cell Biochem. Funct.* **25**, 305-315, (2007).

24 Ly, L. H., Smith, R., Switzer, K. C., Chapkin, R. S. & McMurray, D. N. Dietary eicosapentaenoic acid modulates CTLA-4 expression in murine CD4+ T-cells. *Prostaglandins Leukot. Essent. Fatty Acids* **74**, 29-37, (2006).

25 Jolly, C. A., Jiang, Y. H., Chapkin, R. S. & McMurray, D. N. Dietary (n-3) polyunsaturated fatty acids suppress murine lymphoproliferation, interleukin-2 secretion, and the formation of diacylglycerol and ceramide. *J. Nutr.* **127**, 37–43, (1997).

26 Merzouk, S. A. *et al.* N-3 polyunsaturated fatty acids modulate in-vitro T cell function in type I diabetic patients. *Lipids* **43**, 485-497, (2008).

27 Bi, X. *et al.* ω-3 polyunsaturated fatty acids ameliorate type 1 diabetes and autoimmunity. *J. Clin. Invest.* **127**, 1757-1771, (2017).

28 Monk, J. M., Hou, T. Y., Turk, H. F., McMurray, D. N. & Chapkin, R. S. n3 PUFAs reduce mouse CD4+ T-cell ex vivo polarization into Th17 cells. *J. Nutr.* **143**, 1501-1508, (2013).

29 Reilly, N. A. *et al.* Oleic acid triggers metabolic rewiring of T cells poising them for T helper 9 differentiation. *iScience* **27**, 109496, (2024).

30 Su, B. *et al.* A DMS shotgun lipidomics workflow application to facilitate high-throughput, comprehensive lipidomics. *J. Am. Soc. Mass Spectrom.* **32**, 2655-2663, (2021).

31 Ghorasaini, M. *et al.* Congruence and complementarity of differential mobility spectrometry and NMR spectroscopy for plasma lipidomics. *Metabolites* **12**, 1030, (2022).

32 van der Vusse, G. J. Albumin as fatty acid transporter. *Drug Metab. Pharmacokinet.* **24**, 300-307, (2009).

33 Ledderose, C., Heyn, J., Limbeck, E. & Kreth, S. Selection of reliable reference genes for quantitative real-time PCR in human T cells and neutrophils. *BMC Res. Notes* **4**, 427, (2011).

34 Love, M. I., Huber, W. & Anders, S. Moderated estimation of fold change and dispersion for RNA-seq data with DESeq2. *Genome Biol.* **15**, 550, (2014).

35 Yu, G., Wang, L. G., Han, Y. & He, Q. Y. clusterProfiler: an R package for comparing biological themes among gene clusters. *OMICS* **16**, 284-287, (2012).

36 Corces, M. R. *et al.* An improved ATAC-seq protocol reduces background and enables interrogation of frozen tissues. *Nat. Methods* **14**, 959-962, (2017).

37 Heinz, S. *et al.* Simple combinations of lineage-determining transcription factors prime cis-regulatory elements required for macrophage and B cell identities. *Mol. Cell* **38**, 576-589, (2010).

38 Phillips, J. E. & Corces, V. G. CTCF: master weaver of the genome. *Cell* **137**, 1194-1211, (2009).

39 Zhao, X., Zhu, S., Peng, W. & Xue, H. H. The interplay of transcription and genome topology programs T cell development and differentiation. *J. Immunol.* **209**, 2269-2278, (2022).

40 Nakayama, T. *et al.* Th2 cells in health and disease. *Annu. Rev. Immunol.* **35**, 53-84, (2017).

41 Angkasekwinai, P. Th9 cells in allergic disease. *Curr. Allergy Asthma Rep.* **19**, 29, (2019).

42 Hsu, F. C. *et al.* An essential role for the transcription factor Runx1 in T cell maturation. *Sci. Rep.* **6**, 23533, (2016).

43 Mosure, S. A., Wilson, A. N. & Solt, L. A. Targeting nuclear receptors for Th17-mediated inflammation: REV-ERBerations of circadian rhythm and metabolism. *Immunometabolism* **4**, (2022).

44 Mammadli, M., Suo, L., Sen, J. M. & Karimi, M. TCF-1 is required for CD4 T cell persistence functions during alloimmunity. *Int. J. Mol. Sci.* **24**, 4326, (2023).

45 Liu, Y. *et al.* FoxA1 directs the lineage and immunosuppressive properties of a novel regulatory T cell population in EAE and MS. *Nat. Med.* **20**, 272-282, (2014).

46 Olshansky, B. *et al.* Mineral oil: safety and use as placebo in REDUCE-IT and other clinical studies. *Eur. Heart J. Suppl.* **22**, 34-48, (2020).

47 Sharretts, J. Endocrinologic and metabolic drugs advisory committee meeting. *FDA Briefing Document* (2019).

48 Briefing Document Vascepa®. *Endocrinologic and metabolic drugs adisory committee* **FDA**, (2019).

49 Assessment report Vazkepa. *Committee for Medicinal Products for Human Use* **EMA**, (2021).

50 Klein, J. & Sato, A. The HLA system. *N. Engl. J. Med.* **343**, 702-709, (2000).

51 Tippalagama, R. *et al.* HLA-DR marks recently divided antigen-specific effector CD4 T cells in active tuberculosis patients. *J. Immunol.* **207**, 523-533, (2021).

52 Chapman, N. M., Boothby, M. R. & Chi, H. Metabolic coordination of T cell quiescence and activation. *Nat. Rev. Immunol.* **20**, 55-70, (2020).

53 Grivel, J. C. *et al.* Activation of T lymphocytes in atherosclerotic plaques. *Arterioscler. Thromb. Vasc. Biol.* **31**, 2929-2937, (2011).

54 de Oliveira Otto, M. C. *et al.* Circulating and dietary omega-3 and omega-6 polyunsaturated fatty acids and incidence of CVD in the multi-ethnic study of atherosclerosis. *J. Am. Heart Assoc.* **2**, 000506, (2013).

55 Zhang, P., Smith, R., Chapkin, R. S. & McMurray, D. N. Dietary (n-3) polyunsaturated fatty acids modulate murine Th1/Th2 balance toward the Th2 pole by suppression of Th1 development. *J. Nutr.* **135**, 1745–1751, (2005).

56 Zhang, P. *et al.* Dietary fish oil inhibits antigen-specific murine Th1 cell development by suppression of clonal expansion. *J. Nutr.* **136**, 2391–2398, (2006).

57 Switzer, K. C., McMurray, D. N., Morris, J. S. & Chapkin, R. S. (n-3) Polyunsaturated fatty acids promote activation-induced cell death in murine T lymphocytes. *J. Nutr.* **133**, 496–503, (2003).

58 Zhang, W. *et al.* IL-9 aggravates the development of atherosclerosis in ApoE2/2 mice. *Cardiovasc. Res.* **106**, 453-464, (2015).

59 Gregersen, I. *et al.* Increased systemic and local interleukin 9 levels in patients with carotid and coronary atherosclerosis. *PLoS One* **8**, 72769, (2013).

60 Li, Q. *et al.* Increased Th9 cells and IL-9 levels accelerate disease progression in experimental atherosclerosis. *Am. J. Transl. Res.* **9**, 1335-1343, (2017).

61 Nguyen, T., Nioi, P. & Pickett, C. B. The Nrf2-antioxidant response element signaling pathway and its activation by oxidative stress. *J. Biol. Chem.* **284**, 13291-13295, (2009).

62 Wang, L. & He, C. Nrf2-mediated anti-inflammatory polarization of macrophages as therapeutic targets for osteoarthritis. *Front. Immunol.* **13**, 967193, (2022).

63 Mansouri, A. *et al.* Antioxidant effects of statins by modulating Nrf2 and Nrf2/HO-1 signaling in different diseases. *J. Clin. Med.* **11**, 1313, (2022).

64 Batty, M., Bennett, M. R. & Yu, E. The role of oxidative stress in atherosclerosis. *Cells* **11**, 3843, (2022).

65 Kanno, T., Nakajima, T., Miyako, K. & Endo, Y. Lipid metabolism in Th17 cell function. *Pharmacol. Ther.* **245**, 108411, (2023).

66 Kidani, Y. & Bensinger, S. J. Reviewing the impact of lipid synthetic flux on Th17 function. *Curr. Opin. Immunol.* **46**, 121-126, (2017).

67 Takeuchi, H. *et al.* Retinoid X receptor agonists modulate Foxp3+ regulatory T cell and Th17 cell differentiation with differential dependence on retinoic acid receptor activation. *J. Immunol.* **191**, 3725-3733, (2013).

68 Laguna-Fernandez, A. *et al.* ERV1/ChemR23 signaling protects against atherosclerosis by modifying oxidized low-density lipoprotein uptake and phagocytosis in macrophages. *Circulation* **138**, 1693-1705, (2018).

# Supplemental information

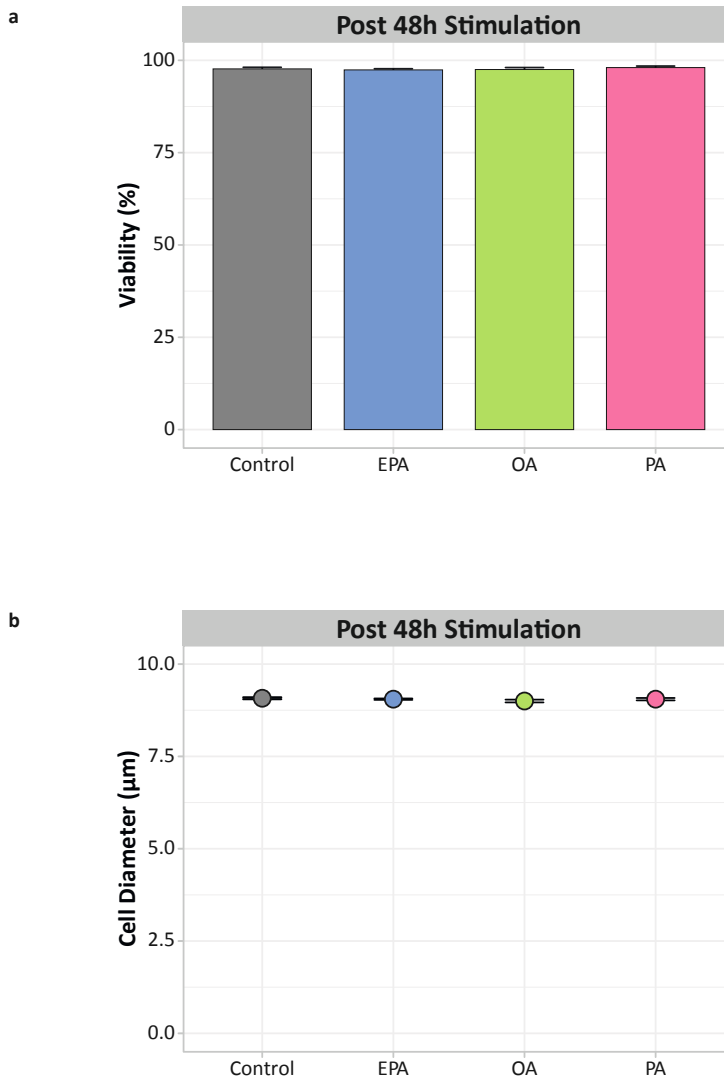


**Supplemental Fig. 1 | Verification of viability and cell diameter post-exposure for RNA sequencing. (a)** Bar plot showing the average cell viability and standard error in percent, as determined by Via1-Cassette™ on a NucleoCounter® NC-200™. On average the cell viability of control exposed cells was 97.7 SE 0.4%, EPA exposed cells was 97.4 SE 0.3% ($p > 0.05$), OA exposed cells was 97.5 SE 0.5% ($p > 0.05$), and PA exposed cells was 98.0 SE 0.4% ($p > 0.05$) at 48h. Thus, there was no effect on $CD4^+$ T cell viability after 48h exposure, n = 8. **(b)** Dot plot showing the average cell diameter and standard error in µm, as determined by Via1-Cassette™ on a NucleoCounter® NC-200™. On average the cell diameter of control exposed cells was 9.1 SE 0.03µm, EPA exposed cells was 9.1 SE 0.02µm ($p > 0.05$), OA exposed cells was 9.0 SE 0.04µm ($p > 0.05$), and PA exposed cells was 9.1 SE 0.03µm ($p > 0.05$) at 48h. Thus, there was no effect on $CD4^+$ T cell diameter after 48h exposure, n = 8. Abbreviations, EPA = eicosapentaenoic acid, h = hours, OA = oleic acid, PA = palmitic acid.

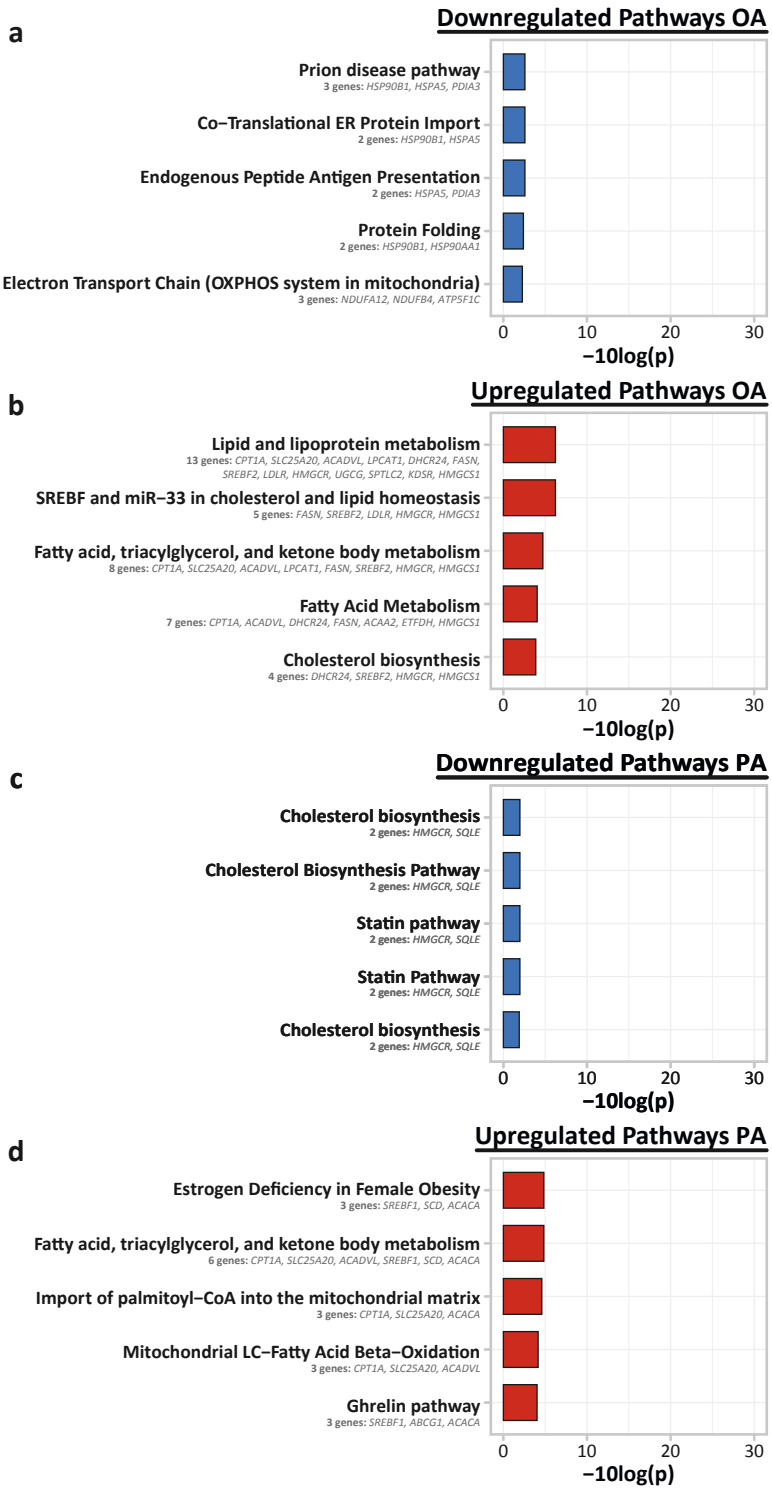
a
Downregulated Pathways OA
Prion disease pathway
3 genes: HSP90B1, HSPA5, PDIA3
Co–Translational ER Protein Import
2 genes: HSP90B1, HSPA5
Endogenous Peptide Antigen Presentation
2 genes: HSPA5, PDIA3
Protein Folding
2 genes: HSP90B1, HSP90AA1
Electron Transport Chain (OXPHOS system in mitochondria)
3 genes: NDUFA12, NDUFB4, ATP5F1C
0
10
20
30
−10log(p)
b
Upregulated Pathways OA
Lipid and lipoprotein metabolism
13 genes: CPT1A, SLC25A20, ACADVL, LPCAT1, DHCR24, FASN, SREBF2, LDLR, HMGCR, UGCG, SPTLC2, KDSR, HMGCS1
SREBF and miR–33 in cholesterol and lipid homeostasis
5 genes: FASN, SREBF2, LDLR, HMGCR, HMGCS1
Fatty acid, triacylglycerol, and ketone body metabolism
8 genes: CPT1A, SLC25A20, ACADVL, LPCAT1, FASN, SREBF2, HMGCR, HMGCS1
Fatty Acid Metabolism
7 genes: CPT1A, ACADVL, DHCR24, FASN, ACAA2, ETFDH, HMGCS1
Cholesterol biosynthesis
4 genes: DHCR24, SREBF2, HMGCR, HMGCS1
0
10
20
30
−10log(p)
c
Downregulated Pathways PA
Cholesterol biosynthesis
2 genes: HMGCR, SQLE
Cholesterol Biosynthesis Pathway
2 genes: HMGCR, SQLE
Statin pathway
2 genes: HMGCR, SQLE
Statin Pathway
2 genes: HMGCR, SQLE
Cholesterol biosynthesis
2 genes: HMGCR, SQLE
0
10
20
30
−10log(p)
d
Upregulated Pathways PA
Estrogen Deficiency in Female Obesity
3 genes: SREBF1, SCD, ACACA
Fatty acid, triacylglycerol, and ketone body metabolism
6 genes: CPT1A, SLC25A20, ACADVL, SREBF1, SCD, ACACA
Import of palmitoyl–CoA into the mitochondrial matrix
3 genes: CPT1A, SLC25A20, ACACA
Mitochondrial LC–Fatty Acid Beta–Oxidation
3 genes: CPT1A, SLC25A20, ACADVL
Ghrelin pathway
3 genes: SREBF1, ABCG1, ACACA
0
10
20
30
−10log(p)

**Supplemental Fig. 2 | Up- and downregulated pathways in PA and OA-exposed non-activated $CD4^+$ T cells.** **(a)** Pathway enrichment analysis of all downregulated OA DEGs generated using *clusterProfiler* using 10 human pathway databases. Top 5 enrichments are shown. **(b)** Pathway enrichment analysis of all upregulated OA DEGs generated using *clusterProfiler* using 10 human pathway databases. Top 5 enrichments are shown. **(c)** Pathway enrichment analysis of all downregulated PA DEGs generated using *clusterProfiler* using 10 human pathway databases. Top 5 enrichments are shown. **(d)** Pathway enrichment analysis of all upregulated PA DEGs generated using *clusterProfiler* using 10 human pathway databases. Top 5 enrichments are shown. Abbreviations, OA = oleic acid, PA = palmitic acid.

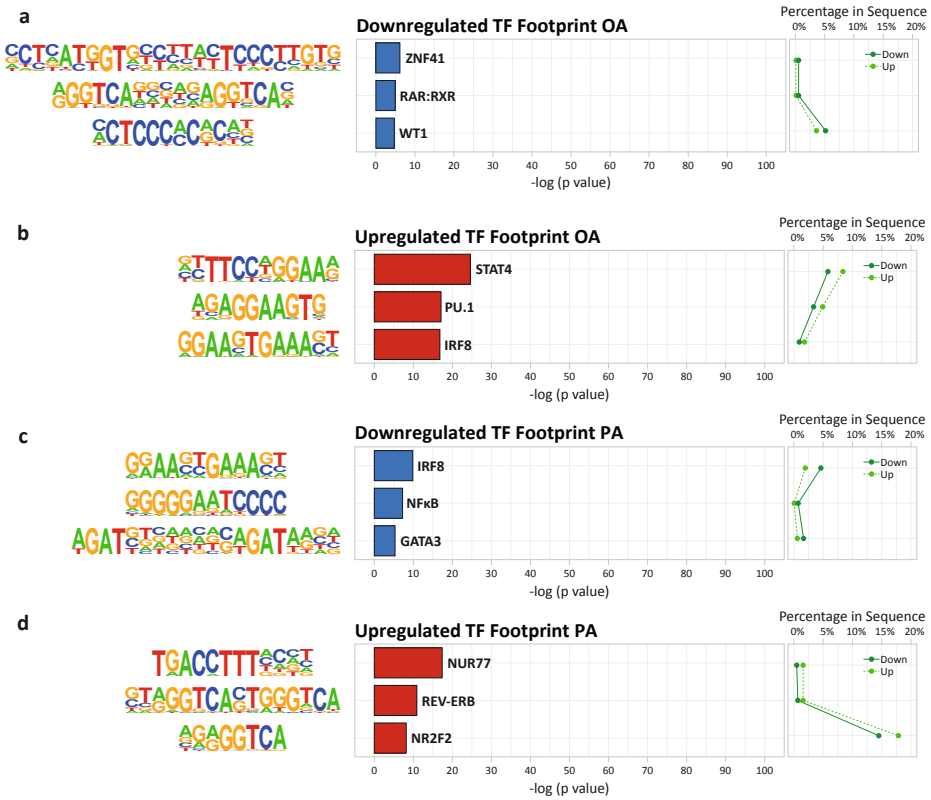


**Supplemental Fig. 3 | Up- and downregulated transcription factors in PA and OA-exposed non-activated CD4+ T cells. (a)** Known motif analysis on promotors of down versus upregulated OA ATAC peaks. Enrichment of transcription factor binding motifs was performed using HOMER. 3 motifs are shown with supplementing information on p-value, percentage of genes in upregulated gene set and percentage of genes in downregulated gene set, transcription factor name, -log(p-value), and percentage in sequence. **(b)** Known motif analysis on promotors of up versus downregulated OA ATAC peaks. Enrichment of transcription factor binding motifs was performed using HOMER. 4 motifs are shown with supplementing information on p-value, percentage of genes in upregulated gene set and percentage of genes in downregulated gene set, transcription factor name, -log(p-value), and percentage in sequence. **(c)** Known motif analysis on promotors of down versus upregulated PA ATAC peaks. Enrichment of transcription factor binding motifs was performed using HOMER. 3 motifs are shown with supplementing information on p-value, percentage of genes in upregulated gene set and percentage of genes in downregulated gene set, transcription factor name, -log(p-value), and percentage in sequence. **(d)** Known motif analysis on promotors of up versus downregulated PA ATAC peaks. Enrichment of transcription factor binding motifs was performed using HOMER. 4 motifs are shown with supplementing information on p-value, percentage of genes in upregulated gene set and percentage of genes in downregulated gene set, transcription factor name, -log(p-value), and percentage in sequence. Abbreviations, OA = oleic acid, PA = palmitic acid, TF = transcription factor.

**Supplemental Table 1 | Changes in gene expression and $CD4^+$ T cell markers due to EPA, PA, or OA exposure.**

**Supplemental Table 1 | (a) (partial)** Downregulated DEGs for EPA exposed non-activated $CD4^+$ T cells in order of significance along with their Ensembl ID, gene symbol, UniProt ID, base mean, log2 fold change, log fold change standard error, p value, and adjusted p value (FDR). Top 30 most significantly expressed genes are shown here.

| Order | Ensembl ID | Gene Symbol | UniProt | baseMean | log2FC | log2FC SE | P value | $P_{FDR}$ |
|---|---|---|---|---|---|---|---|---|
| 1 | ENSG00000026025 | *VIM* | P08670 | 10461.483 | -0.686 | 0.075 | 4.44E-20 | 1.44E-16 |
| 2 | ENSG00000205542 | *TMSB4X* | P62328 | 48176.611 | -0.577 | 0.072 | 7.52E-16 | 1.08E-12 |
| 3 | ENSG00000204287 | *HLA-DRA* | P01903 | 633.049 | -1.137 | 0.147 | 1.27E-14 | 1.32E-11 |
| 4 | ENSG00000138326 | *RPS24* | P62847 | 18476.569 | -0.730 | 0.095 | 1.33E-14 | 1.32E-11 |
| 5 | ENSG00000231389 | *HLA-DPA1* | P20036 | 417.419 | -0.963 | 0.130 | 1.43E-13 | 1.16E-10 |
| 6 | ENSG00000026950 | *BTN3A1* | O00481 | 2825.734 | -0.939 | 0.131 | 7.52E-13 | 5.12E-10 |
| 7 | ENSG00000106952 | *TNFSF8* | P32971 | 1146.126 | -0.816 | 0.114 | 9.00E-13 | 5.83E-10 |
| 8 | ENSG00000034510 | *TMSB10* | P63313 | 16350.584 | -0.622 | 0.092 | 1.37E-11 | 6.08E-09 |
| 9 | ENSG00000118181 | *RPS25* | P62851 | 30745.712 | -0.533 | 0.079 | 1.41E-11 | 6.08E-09 |
| 10 | ENSG00000223865 | *HLA-DPB1* | P04440 | 318.848 | -1.159 | 0.174 | 2.74E-11 | 1.11E-08 |
| 11 | ENSG00000186470 | *BTN3A2* | P78410 | 3097.909 | -0.814 | 0.125 | 7.80E-11 | 2.65E-08 |
| 12 | ENSG00000240065 | *PSMB9* | P28065 | 851.254 | -0.822 | 0.127 | 1.09E-10 | 3.44E-08 |
| 13 | ENSG00000111801 | *BTN3A3* | O00478 | 2129.494 | -0.732 | 0.114 | 1.32E-10 | 4.08E-08 |
| 14 | ENSG00000100097 | *LGALS1* | P09382 | 476.452 | -0.723 | 0.113 | 1.68E-10 | 4.93E-08 |
| 15 | ENSG00000204592 | *HLA-E* | P13747 | 21754.754 | -0.713 | 0.112 | 1.76E-10 | 4.96E-08 |
| 16 | ENSG00000255150 | *EID3* | Q8N140 | 109.010 | -1.274 | 0.200 | 1.76E-10 | 4.96E-08 |
| 17 | ENSG00000120833 | *SOCS2* | O14508 | 272.816 | -0.932 | 0.147 | 2.27E-10 | 6.12E-08 |
| 18 | ENSG00000160856 | *FCRL3* | Q96P31 | 201.018 | -1.190 | 0.189 | 3.06E-10 | 7.76E-08 |
| 19 | ENSG00000019582 | *CD74* | P04233 | 2645.553 | -0.622 | 0.099 | 3.92E-10 | 9.74E-08 |
| 20 | ENSG00000008517 | *IL32* | P24001 | 4786.915 | -0.671 | 0.107 | 4.11E-10 | 1.00E-07 |
| 21 | ENSG00000185880 | *TRIM69* | Q86WT6 | 867.798 | -0.572 | 0.092 | 5.10E-10 | 1.22E-07 |
| 22 | ENSG00000131981 | *LGALS3* | P17931 | 568.618 | -0.653 | 0.107 | 9.88E-10 | 2.28E-07 |
| 23 | ENSG00000113088 | *GZMK* | P49863 | 365.982 | -1.139 | 0.187 | 1.02E-09 | 2.31E-07 |

*[continued on next page]*

**Supplemental Table 1 | (a) (partial)** *[continued]*

| Order | Ensembl ID | Gene Symbol | UniProt | baseMean | log2FC | log2FC SE | P value | $P_{FDR}$ |
|---|---|---|---|---|---|---|---|---|
| 24 | ENSG00000107736 | *CDH23* | Q9H251 | 268.652 | -1.072 | 0.177 | 1.35E-09 | 3.02E-07 |
| 25 | ENSG00000243335 | *KCTD7* | Q96MP8 | 1002.502 | -0.512 | 0.085 | 1.40E-09 | 3.07E-07 |
| 26 | ENSG00000114737 | *CISH* | Q9NSE2 | 599.263 | -0.822 | 0.137 | 2.18E-09 | 4.55E-07 |
| 27 | ENSG00000196126 | *HLA-DRB1* | P01911 | 300.924 | -1.002 | 0.168 | 2.43E-09 | 5.00E-07 |
| 28 | ENSG00000130755 | *GMFG* | O60234 | 3215.210 | -0.548 | 0.092 | 2.54E-09 | 5.14E-07 |
| 29 | ENSG00000143947 | *RPS27A* | P62979 | 45091.864 | -0.408 | 0.069 | 3.60E-09 | 6.96E-07 |
| 30 | ENSG00000101608 | *MYL12A* | P19105 | 7915.620 | -0.504 | 0.086 | 3.78E-09 | 7.19E-07 |

**Supplemental Table 1 | (b) (partial)** Upregulated DEGs for EPA exposed non-activated CD4+ T cells in order of significance along with their Ensembl ID, gene symbol, UniProt ID, base mean, log2 fold change, log fold change standard error, p value, and adjusted p value (FDR). Top 30 most significantly expressed genes are shown here.



| Order | Ensembl ID | Gene Symbol | UniProt | baseMean | log2FC | log2FC SE | P value | $P_{FDR}$ |
|---|---|---|---|---|---|---|---|---|
| 1 | ENSG00000181019 | *NQO1* | P15559 | 346.693 | 2.457 | 0.218 | 2.37E-29 | 3.07E-25 |
| 2 | ENSG00000113369 | *ARRDC3* | Q96B67 | 3175.559 | 1.305 | 0.118 | 2.59E-28 | 1.68E-24 |
| 3 | ENSG00000110090 | *CPT1A* | P50416 | 603.707 | 2.716 | 0.270 | 8.52E-24 | 3.68E-20 |
| 4 | ENSG00000103257 | *SLC7A5* | Q01650 | 1346.098 | 1.219 | 0.133 | 5.98E-20 | 1.55E-16 |
| 5 | ENSG00000115758 | *ODC1* | P11926 | 1660.221 | 1.023 | 0.120 | 1.56E-17 | 3.37E-14 |
| 6 | ENSG00000178537 | *SLC25A20* | O43772 | 267.897 | 1.144 | 0.136 | 3.55E-17 | 6.57E-14 |
| 7 | ENSG00000090861 | *AARS1* | P49588 | 4381.327 | 0.697 | 0.084 | 7.34E-17 | 1.19E-13 |
| 8 | ENSG00000135069 | *PSAT1* | Q9Y617 | 1488.575 | 1.086 | 0.136 | 1.18E-15 | 1.53E-12 |
| 9 | ENSG00000001084 | *GCLC* | P48506 | 1258.380 | 0.872 | 0.109 | 1.31E-15 | 1.54E-12 |
| 10 | ENSG00000167703 | *SLC43A2* | Q8N370 | 169.252 | 2.053 | 0.273 | 5.60E-14 | 5.17E-11 |
| 11 | ENSG00000125534 | *PPDPF* | Q9H3Y8 | 1332.610 | 0.876 | 0.118 | 9.86E-14 | 8.50E-11 |
| 12 | ENSG00000172613 | *RAD9A* | Q99638 | 820.146 | 0.823 | 0.113 | 3.95E-13 | 3.01E-10 |
| 13 | ENSG00000139514 | *SLC7A1* | P30825 | 1604.807 | 0.522 | 0.073 | 6.51E-13 | 4.68E-10 |

*[continued on next page]*

**Supplemental Table 1 | (b) (partial)** *[continued]*

| Order | Ensembl ID | Gene Symbol | UniProt | baseMean | log2FC | log2FC SE | P value | $P_{FDR}$ |
|---|---|---|---|---|---|---|---|---|
| 14 | ENSG00000051108 | *HERPUD1* | Q15011 | 1950.929 | 0.623 | 0.087 | 1.07E-12 | 6.59E-10 |
| 15 | ENSG00000197063 | *MAFG* | O15525 | 646.794 | 1.042 | 0.148 | 1.68E-12 | 9.53E-10 |
| 16 | ENSG00000116852 | *KIF21B* | O75037 | 5536.202 | 0.782 | 0.111 | 1.69E-12 | 9.53E-10 |
| 17 | ENSG00000100292 | *HMOX1* | P09601 | 118.300 | 4.091 | 0.583 | 2.20E-12 | 1.19E-09 |
| 18 | ENSG00000198830 | *HMGN2* | P05204 | 4201.608 | 0.462 | 0.066 | 2.80E-12 | 1.45E-09 |
| 19 | ENSG00000113407 | *TARS1* | P26639 | 3883.418 | 0.621 | 0.090 | 4.95E-12 | 2.46E-09 |
| 20 | ENSG00000162413 | *KLHL21* | Q9UJP4 | 1585.720 | 0.772 | 0.112 | 5.78E-12 | 2.77E-09 |
| 21 | ENSG00000168003 | *SLC3A2* | P08195 | 5743.672 | 1.397 | 0.204 | 7.76E-12 | 3.58E-09 |
| 22 | ENSG00000072778 | *ACADVL* | P49748 | 3071.367 | 0.541 | 0.081 | 2.37E-11 | 9.91E-09 |
| 23 | ENSG00000196305 | *IARS1* | P41252 | 3525.848 | 0.446 | 0.067 | 3.64E-11 | 1.43E-08 |
| 24 | ENSG00000128965 | *CHAC1* | Q9BUX1 | 266.899 | 1.461 | 0.221 | 4.02E-11 | 1.53E-08 |
| 25 | ENSG00000082898 | *XPO1* | O14980 | 4845.018 | 0.824 | 0.126 | 5.09E-11 | 1.88E-08 |
| 26 | ENSG00000139112 | *GABARAPL1* | Q9H0R8 | 821.575 | 1.034 | 0.158 | 6.32E-11 | 2.27E-08 |
| 27 | ENSG00000087086 | *FTL* | P02792 | 23835.068 | 0.800 | 0.123 | 6.97E-11 | 2.44E-08 |
| 28 | ENSG00000134294 | *SLC38A2* | Q96QD8 | 5627.146 | 0.676 | 0.104 | 9.33E-11 | 3.10E-08 |
| 29 | ENSG00000166986 | *MARS1* | P56192 | 5359.986 | 0.444 | 0.069 | 1.00E-10 | 3.24E-08 |
| 30 | ENSG00000198743 | *SLC5A3* | P53794 | 1939.433 | 0.860 | 0.135 | 1.66E-10 | 4.93E-08 |

**Supplemental Table 1 | (c)** Downregulated DEGs for OA exposed non-activated $CD4^+$ T cells in order of significance along with their Ensembl ID, gene symbol, UniProt ID, base mean, log2 fold change, log fold change standard error, p value, and adjusted p value (FDR).

| Order | Ensembl ID | Gene Symbol | UniProt | baseMean | log2FC | log2FC SE | P value | $P_{FDR}$ |
|---|---|---|---|---|---|---|---|---|
| 1 | ENSG00000205542 | *TMSB4X* | P62328 | 53784.953 | -0.300 | 0.063 | 1.93E-06 | 0.00146 |
| 2 | ENSG00000166598 | *HSP90B1* | P14625 | 9262.938 | -0.336 | 0.071 | 2.02E-06 | 0.00146 |
| 3 | ENSG00000044574 | *HSPA5* | P11021 | 5535.011 | -0.382 | 0.081 | 2.19E-06 | 0.00149 |
| 4 | ENSG00000184752 | *NDUFA12* | Q9UI09 | 1467.880 | -0.347 | 0.082 | 2.55E-05 | 0.01178 |
| 5 | ENSG00000111348 | *ARHGDIB* | P52566 | 18341.064 | -0.224 | 0.057 | 9.10E-05 | 0.03021 |

*[continued on next page]*

**Supplemental Table 1 | (c)** *[continued]*

| Order | Ensembl ID | Gene Symbol | UniProt | baseMean | log2FC | log2FC SE | P value | $P_{FDR}$ |
|---|---|---|---|---|---|---|---|---|
| 6 | ENSG00000065518 | *NDUFB4* | O95168 | 923.826 | -0.345 | 0.090 | 0.000119 | 0.03589 |
| 7 | ENSG00000167004 | *PDIA3* | P30101 | 5053.715 | -0.275 | 0.072 | 0.000135 | 0.03820 |
| 8 | ENSG00000034510 | *TMSB10* | P63313 | 18121.778 | -0.287 | 0.076 | 0.000146 | 0.03951 |
| 9 | ENSG00000265972 | *TXNIP* | Q9H3M7 | 19375.847 | -0.185 | 0.049 | 0.000150 | 0.03973 |
| 10 | ENSG00000145050 | *MANF* | P55145 | 661.685 | -0.427 | 0.113 | 0.000159 | 0.04114 |
| 11 | ENSG00000111481 | *COPZ1* | P61923 | 1920.473 | -0.221 | 0.060 | 0.000207 | 0.04787 |
| 12 | ENSG00000165629 | *ATP5F1C* | P36542 | 1803.183 | -0.277 | 0.075 | 0.000211 | 0.04787 |
| 13 | ENSG00000080824 | *HSP90AA1* | P07900 | 12647.574 | -0.264 | 0.072 | 0.000222 | 0.04787 |

**Supplemental Table 1 | (d) (partial)** Upregulated DEGs for OA exposed non-activated CD4+ T cells in order of significance along with their Ensembl ID, gene symbol, UniProt ID, base mean, log2 fold change, log fold change standard error, p value, and adjusted p value (FDR). Top 30 most significantly expressed genes are shown here.

| Order | Ensembl ID | Gene Symbol | UniProt | baseMean | log2FC | log2FC SE | P value | $P_{FDR}$ |
|---|---|---|---|---|---|---|---|---|
| 1 | ENSG00000110090 | *CPT1A* | P50416 | 893.439 | 3.460 | 0.110 | 2.87E-218 | 3.71E-214 |
| 2 | ENSG00000178537 | *SLC25A20* | O43772 | 352.353 | 1.669 | 0.121 | 1.34E-43 | 8.65E-40 |
| 3 | ENSG00000145860 | *RNF145* | Q96MT1 | 2335.306 | 0.638 | 0.068 | 7.35E-21 | 3.17E-17 |
| 4 | ENSG00000072778 | *ACADVL* | P49748 | 3128.902 | 0.557 | 0.064 | 2.87E-18 | 9.28E-15 |
| 5 | ENSG00000143110 | *C1orf162* | Q8NEQ5 | 1332.128 | 0.522 | 0.072 | 3.78E-13 | 9.78E-10 |
| 6 | ENSG00000153395 | *LPCAT1* | Q8NF37 | 1527.598 | 0.473 | 0.067 | 1.35E-12 | 2.59E-09 |
| 7 | ENSG00000184602 | *SNN* | O75324 | 905.754 | 0.581 | 0.082 | 1.40E-12 | 2.59E-09 |
| 8 | ENSG00000116133 | *DHCR24* | Q15392 | 474.003 | 0.588 | 0.093 | 3.08E-10 | 4.98E-07 |
| 9 | ENSG00000169710 | *FASN* | P49327 | 866.664 | 0.680 | 0.116 | 4.68E-09 | 6.74E-06 |
| 10 | ENSG00000198911 | *SREBF2* | Q12772 | 3184.981 | 0.390 | 0.070 | 2.37E-08 | 3.07E-05 |
| 11 | ENSG00000102032 | *RENBP* | P51606 | 250.558 | 0.747 | 0.142 | 1.57E-07 | 0.000184 |
| 12 | ENSG00000130164 | *LDLR* | P01130 | 1013.144 | 0.461 | 0.088 | 1.87E-07 | 0.000202 |
| 13 | ENSG00000167315 | *ACAA2* | P42765 | 483.439 | 0.558 | 0.108 | 2.23E-07 | 0.000222 |

*[continued on next page]*

**Supplemental Table 1 | (d) (partial)** *[continued]*

| Order | Ensembl ID | Gene Symbol | UniProt | baseMean | log2FC | log2FC SE | P value | $P_{FDR}$ |
|---|---|---|---|---|---|---|---|---|
| 14 | ENSG00000166575 | *TMEM135* | Q86UB9 | 161.166 | 0.722 | 0.146 | 7.39E-07 | 0.000683 |
| 15 | ENSG00000167106 | *FAM102A* | Q5T9C2 | 7915.593 | 0.290 | 0.060 | 1.43E-06 | 0.001236 |
| 16 | ENSG00000103249 | *CLCN7* | P51798 | 1764.038 | 0.411 | 0.086 | 1.88E-06 | 0.001456 |
| 17 | ENSG00000069424 | *KCNAB2* | Q13303 | 4855.716 | 0.308 | 0.065 | 2.30E-06 | 0.001489 |
| 18 | ENSG00000113161 | *HMGCR* | P04035 | 913.374 | 0.369 | 0.081 | 5.52E-06 | 0.003402 |
| 19 | ENSG00000198355 | *PIM3* | Q86V86 | 716.562 | 0.450 | 0.102 | 1.05E-05 | 0.006197 |
| 20 | ENSG00000171503 | *ETFDH* | Q16134 | 301.259 | 0.553 | 0.127 | 1.41E-05 | 0.007922 |
| 21 | ENSG00000140526 | *ABHD2* | P08910 | 1283.746 | 0.291 | 0.068 | 1.70E-05 | 0.009194 |
| 22 | ENSG00000174903 | *RAB1B* | Q9H0U4 | 2107.877 | 0.334 | 0.078 | 1.95E-05 | 0.010094 |
| 23 | ENSG00000106266 | *SNX8* | Q9Y5X2 | 144.357 | 0.710 | 0.168 | 2.40E-05 | 0.011780 |
| 24 | ENSG00000079432 | *CIC* | Q96RK0 | 2107.033 | 0.347 | 0.082 | 2.53E-05 | 0.011780 |
| 25 | ENSG00000163162 | *RNF149* | Q8NC42 | 1907.621 | 0.340 | 0.081 | 3.02E-05 | 0.013471 |
| 26 | ENSG00000161011 | *SQSTM1* | Q13501 | 3912.137 | 0.262 | 0.063 | 3.26E-05 | 0.014059 |
| 27 | ENSG00000172059 | *KLF11* | O14901 | 161.305 | 0.718 | 0.174 | 3.65E-05 | 0.015237 |
| 28 | ENSG00000158470 | *B4GALT5* | O43286 | 294.347 | 0.478 | 0.120 | 6.72E-05 | 0.026870 |
| 29 | ENSG00000011021 | *CLCN6* | P51797 | 556.903 | 0.388 | 0.098 | 6.85E-05 | 0.026870 |
| 30 | ENSG00000113163 | *CERT1* | Q9Y5P4 | 911.346 | 0.347 | 0.088 | 7.53E-05 | 0.028490 |

**Supplemental Table 1 | (e)** Downregulated DEGs for PA exposed non-activated $CD4^+$ T cells in order of significance along with their Ensembl ID, gene symbol, UniProt ID, base mean, log2 fold change, log fold change standard error, p value, and adjusted p value (FDR).

| Order | Ensembl ID | Gene Symbol | UniProt | baseMean | log2FC | log2FC SE | P value | $P_{FDR}$ |
|---|---|---|---|---|---|---|---|---|
| 1 | ENSG00000117632 | *STMN1* | P16949 | 1324.856 | -0.407 | 0.067 | 1.44E-09 | 2.68E-06 |
| 2 | ENSG00000163659 | *TIPARP* | Q7Z3E1 | 2383.237 | -0.329 | 0.058 | 1.57E-08 | 2.04E-05 |
| 3 | ENSG00000153395 | *LPCAT1* | Q8NF37 | 1166.324 | -0.276 | 0.058 | 2.38E-06 | 0.00257 |
| 4 | ENSG00000113161 | *HMGCR* | P04035 | 726.112 | -0.325 | 0.070 | 3.58E-06 | 0.00328 |
| 5 | ENSG00000118816 | *CCNI* | Q14094 | 4732.443 | -0.218 | 0.047 | 3.99E-06 | 0.00328 |

*[continued on next page]*

**Supplemental Table 1 | (e)** *[continued]*

| Order | Ensembl ID | Gene Symbol | UniProt | baseMean | log2FC | log2FC SE | P value | $P_{FDR}$ |
|---|---|---|---|---|---|---|---|---|
| 6 | ENSG00000145741 | *BTF3* | P20290 | 10617.724 | -0.255 | 0.056 | 4.30E-06 | 0.00328 |
| 7 | ENSG00000006451 | *RALA* | P11233 | 1137.560 | -0.283 | 0.067 | 2.66E-05 | 0.01724 |
| 8 | ENSG00000145860 | *RNF145* | Q96MT1 | 1666.498 | -0.287 | 0.069 | 2.81E-05 | 0.01733 |
| 9 | ENSG00000187109 | *NAP1L1* | P55209 | 12784.530 | -0.322 | 0.077 | 3.00E-05 | 0.01768 |
| 10 | ENSG00000128989 | *ARPP19* | P56211 | 1868.746 | -0.278 | 0.067 | 3.43E-05 | 0.01932 |
| 11 | ENSG00000104549 | *SQLE* | Q14534 | 334.452 | -0.364 | 0.090 | 4.68E-05 | 0.02427 |
| 12 | ENSG00000117592 | *PRDX6* | P30041 | 1454.171 | -0.211 | 0.053 | 7.87E-05 | 0.03518 |
| 13 | ENSG00000153283 | *CD96* | P40200 | 6532.967 | -0.210 | 0.054 | 0.000104 | 0.04298 |
| 14 | ENSG00000130741 | *EIF2S3* | P41091 | 5440.858 | -0.211 | 0.055 | 0.000107 | 0.04298 |
| 15 | ENSG00000125868 | *DSTN* | P60981 | 923.114 | -0.270 | 0.070 | 0.000109 | 0.04298 |

**Supplemental Table 1 | (f)** Upregulated DEGs for PA exposed non-activated $CD4^+$ T cells in order of significance along with their Ensembl ID, gene symbol, UniProt ID, base mean, log2 fold change, log fold change standard error, p value, and adjusted p value (FDR).

| Order | Ensembl ID | Gene Symbol | UniProt | baseMean | log2FC | log2FC SE | P value | $P_{FDR}$ |
|---|---|---|---|---|---|---|---|---|
| 1 | ENSG00000110090 | *CPT1A* | P50416 | 709.522 | 3.173 | 0.112 | 1.88E-177 | 2.44E-173 |
| 2 | ENSG00000178537 | *SLC25A20* | O43772 | 328.362 | 1.552 | 0.099 | 1.28E-55 | 8.30E-52 |
| 3 | ENSG00000072778 | *ACADVL* | P49748 | 3226.461 | 0.642 | 0.055 | 3.26E-31 | 1.41E-27 |
| 4 | ENSG00000072310 | *SREBF1* | P36956 | 748.306 | 1.252 | 0.125 | 1.23E-23 | 3.99E-20 |
| 5 | ENSG00000143110 | *C1orf162* | Q8NEQ5 | 1302.359 | 0.464 | 0.058 | 1.83E-15 | 4.76E-12 |
| 6 | ENSG00000111684 | *LPCAT3* | Q6P1A2 | 415.027 | 0.690 | 0.109 | 2.26E-10 | 4.89E-07 |
| 7 | ENSG00000160179 | *ABCG1* | P45844 | 158.548 | 1.060 | 0.176 | 1.75E-09 | 2.84E-06 |
| 8 | ENSG00000167315 | *ACAA2* | P42765 | 486.997 | 0.560 | 0.095 | 3.79E-09 | 5.47E-06 |
| 9 | ENSG00000166575 | *TMEM135* | Q86UB9 | 164.063 | 0.743 | 0.148 | 5.64E-07 | 0.000665 |
| 10 | ENSG00000149428 | *HYOU1* | Q9Y4L1 | 2099.100 | 0.321 | 0.069 | 3.85E-06 | 0.003283 |
| 11 | ENSG00000099194 | *SCD* | O00767 | 183.550 | 0.595 | 0.129 | 4.11E-06 | 0.003283 |

*[continued on next page]*

**Supplemental Table 1 | (f)** *[continued]*

| Order | Ensembl ID | Gene Symbol | UniProt | baseMean | log2FC | log2FC SE | P value | $P_{FDR}$ |
|---|---|---|---|---|---|---|---|---|
| 12 | ENSG00000196155 | *PLEKHG4* | Q58EX7 | 674.104 | 0.305 | 0.072 | 2.22E-05 | 0.015991 |
| 13 | ENSG00000182871 | *COL18A1* | P39060 | 687.338 | 0.507 | 0.120 | 2.49E-05 | 0.016984 |
| 14 | ENSG00000278540 | *ACACA* | Q13085 | 410.104 | 0.359 | 0.088 | 4.54E-05 | 0.024270 |
| 15 | ENSG00000141524 | *TMC6* | Q7Z403 | 9025.505 | 0.274 | 0.068 | 5.20E-05 | 0.025954 |
| 16 | ENSG00000079432 | *CIC* | Q96RK0 | 2111.939 | 0.362 | 0.091 | 7.28E-05 | 0.034997 |
| 17 | ENSG00000182095 | *TNRC18* | O15417 | 1055.115 | 0.343 | 0.087 | 7.56E-05 | 0.035038 |
| 18 | ENSG00000155090 | *KLF10* | Q13118 | 39.296 | 1.179 | 0.302 | 9.28E-05 | 0.040127 |

**Supplemental Table 1 | (g)** Table showing additional information on the genes that overlap between the different fatty acids. Information on Gene Symbol, Ensembl ID, chromosome location, log2 fold change of that gene in each specific fatty acid, p value of that gene in each specific fatty acid, adjusted p value of that gene in each specific fatty acid, and whether the direction of gene expression is the same in each fatty acid is included.

| Overlapping Genes | Ensembl ID | log2FC EPA | log2FC OA | log2FC PA | P value EPA | P value OA | P value PA | $P_{FDR}$ EPA | $P_{FDR}$ OA | $P_{FDR}$ PA | Direction Same |
|---|---|---|---|---|---|---|---|---|---|---|---|
| **Overlapping Genes EPA vs OA vs PA** | | | | | | | | | | | |
| *CPT1A* | ENSG00000110090 | 2.716 | 3.460 | 3.173 | 8.52E-24 | 2.87E-218 | 1.88E-177 | 3.68E-20 | 3.71E-214 | 2.44E-173 | Yes Up |
| *SLC25A20* | ENSG00000178537 | 1.144 | 1.669 | 1.552 | 3.55E-17 | 1.34E-43 | 1.28E-55 | 6.57E-14 | 8.65E-40 | 8.30E-52 | Yes Up |
| *ACADVL* | ENSG00000072778 | 0.541 | 0.557 | 0.642 | 2.37E-11 | 2.87E-18 | 3.26E-31 | 9.91E-09 | 9.28E-15 | 1.41E-27 | Yes Up |
| *ACAA2* | ENSG00000167315 | 0.340 | 0.558 | 0.560 | 0.00177 | 2.23E-07 | 3.79E-09 | 0.02553 | 0.00022 | 5.47E-06 | Yes Up |
| **Overlapping Genes EPA vs OA** | | | | | | | | | | | |
| *TMSB4X* | ENSG00000205542 | -0.577 | -0.300 | | 7.52E-16 | 1.93E-06 | | 1.08E-12 | 0.00146 | | Yes Down |
| *PPDPF* | ENSG00000125534 | 0.876 | 0.298 | | 9.86E-14 | 0.00017 | | 8.50E-11 | 0.04178 | | Yes Up |
| *TMSB10* | ENSG00000034510 | -0.622 | -0.287 | | 1.37E-11 | 0.00015 | | 6.08E-09 | 0.03951 | | Yes Down |
| *CLCN7* | ENSG00000103249 | 0.599 | 0.411 | | 1.76E-09 | 1.88E-06 | | 3.74E-07 | 0.00146 | | Yes Up |
| *ETFDH* | ENSG00000171503 | 0.758 | 0.553 | | 1.98E-08 | 1.41E-05 | | 2.84E-06 | 0.00792 | | Yes Up |
| *SQSTM1* | ENSG00000161011 | 0.618 | 0.262 | | 4.20E-08 | 3.26E-05 | | 5.49E-06 | 0.01406 | | Yes Up |
| *RENBP* | ENSG00000102032 | 0.716 | 0.747 | | 8.37E-06 | 1.57E-07 | | 0.00042 | 0.00018 | | Yes Up |
| *PIM3* | ENSG00000198355 | 0.479 | 0.450 | | 2.24E-05 | 1.05E-05 | | 0.00091 | 0.00620 | | Yes Up |

*[continued on next page]*

**Supplemental Table 1 | (g)** *[continued]*

| Overlapping Genes | Ensembl ID | log2FC EPA | log2FC OA | log2FC PA | P value EPA | P value OA | P value PA | $P_{FDR}$ EPA | $P_{FDR}$ OA | $P_{FDR}$ PA | Direction Same |
|---|---|---|---|---|---|---|---|---|---|---|---|
| *TXNIP* | ENSG00000265972 | -0.278 | -0.185 | | 2.93E-05 | 0.00015 | | 0.00113 | 0.03973 | | Yes Down |
| *CLCN6* | ENSG00000011021 | 0.522 | 0.388 | | 4.06E-05 | 6.85E-05 | | 0.00147 | 0.02687 | | Yes Up |
| *FLCN* | ENSG00000154803 | 0.348 | 0.260 | | 4.13E-05 | 9.78E-05 | | 0.00149 | 0.03165 | | Yes Up |
| *AMDHD2* | ENSG00000162066 | 0.537 | 0.482 | | 0.00012 | 8.14E-05 | | 0.00352 | 0.02849 | | Yes Up |
| *PPP1R15A* | ENSG00000087074 | 0.459 | 0.344 | | 0.00023 | 0.00022 | | 0.00547 | 0.04787 | | Yes Up |
| *HSP90B1* | ENSG00000166598 | -0.305 | -0.336 | | 0.00035 | 2.02E-06 | | 0.00764 | 0.00146 | | Yes Down |
| *ARHGDIB* | ENSG00000111348 | -0.247 | -0.224 | | 0.00067 | 9.10E-05 | | 0.01230 | 0.03021 | | Yes Down |
| *SNX8* | ENSG00000106266 | 0.576 | 0.710 | | 0.00124 | 2.40E-05 | | 0.01963 | 0.01178 | | Yes Up |
| *ATXN2L* | ENSG00000168488 | 0.264 | 0.254 | | 0.00133 | 0.00022 | | 0.02050 | 0.04787 | | Yes Up |
| *HSPA5* | ENSG00000044574 | -0.237 | -0.382 | | 0.00197 | 2.19E-06 | | 0.02764 | 0.00149 | | Yes Down |
| **Overlapping Genes EPA vs PA** | | | | | | | | | | | |
| *CD96* | ENSG00000153283 | -0.419 | | -0.210 | 6.55E-08 | | 0.00010 | 7.70E-06 | | 0.04298 | Yes Down |
| *TNRC18* | ENSG00000182095 | 0.355 | | 0.343 | 0.00012 | | 7.56E-05 | 0.00353 | | 0.03504 | Yes Up |
| *PLEKHG4* | ENSG00000196155 | -0.417 | | 0.305 | 0.00128 | | 2.22E-05 | 0.02012 | | 0.01599 | No EPA Down PA Up |

*[continued on next page]*

**Supplemental Table 1 | (g)** *[continued]*

| Overlapping Genes | Ensembl ID | log2FC EPA | log2FC OA | log2FC PA | P value EPA | P value OA | P value PA | $P_{FDR}$ EPA | $P_{FDR}$ OA | $P_{FDR}$ PA | Direction Same |
|---|---|---|---|---|---|---|---|---|---|---|---|
| *COL18A1* | ENSG00000182871 | -0.565 | | 0.507 | 0.00196 | | 2.49E-05 | 0.02757 | | 0.01698 | Yes Up |
| **Overlapping Genes OA vs PA** | | | | | | | | | | | |
| *RNF145* | ENSG00000145860 | | 0.638 | -0.287 | | 7.35E-21 | 2.81E-05 | | 3.17E-17 | 0.01733 | No OA Up PA Down |
| *C1orf162* | ENSG00000143110 | | 0.522 | 0.464 | | 3.78E-13 | 1.83E-15 | | 9.78E-10 | 4.76E-12 | Yes Up |
| *LPCAT1* | ENSG00000111684 | | 0.473 | 0.690 | | 1.35E-12 | 2.26E-10 | | 2.59E-09 | 4.89E-07 | Yes Up |
| *TMEM135* | ENSG00000166575 | | 0.722 | 0.743 | | 7.39E-07 | 5.64E-07 | | 0.00068 | 0.00067 | Yes Up |
| *HMGCR* | ENSG00000113161 | | 0.369 | -0.325 | | 5.52E-06 | 3.58E-06 | | 0.00340 | 0.00328 | No OA Up PA Down |
| *CIC* | ENSG00000079432 | | 0.347 | 0.362 | | 2.53E-05 | 7.28E-05 | | 0.01178 | 0.03500 | Yes Up |
| *KLF10* | ENSG00000155090 | | 1.297 | 1.179 | | 0.00017 | 9.28E-05 | | 0.04178 | 0.04013 | Yes Up |

**Supplemental Table 1 | (h) (partial)** Pathway enrichment analysis of all downregulated EPA DEGs generated using *clusterProfiler* using 10 human pathway databases. Enriched pathways are shown with information on which group that term clusters into based on the Jaccard index > 0.70, pathway term, number of DEGs that overlap with that databases gene set for that pathway, p value, adjusted p value, number of DEGs in that pathway that were upregulated, number of DEGs in that pathway that were downregulated, and gene names of all DEGs included in that pathway. Only the top term of the first 20 groups are shown here.

| Group | Term | Overlap | P value | Adjusted P value | Up-regulated | Down-regulated | Genes |
|---|---|---|---|---|---|---|---|
| 1 | Eukaryotic translation elongation | 44/85 | 7.47E-31 | 1.75E-27 | 0 | 44 | *RPS24, RPS25, RPS27A, RPL35A, RPS12, RPS15A, RPL30, RPL34, RPS6, RPL23, RPS29, RPL31, RPS7, RPS21, RPS20, RPS23, RPS8, RPS13, RPL21, RPL37, RPL23A, RPL11, RPS27, RPL32, RPL27, RPS3A, EEF1B2, RPL39, RPL38, RPL12, RPL4, RPL10A, RPL41, RPL37A, RPL9, RPL5, RPL24, RPL6, RPL19, UBA52, RPS11, RPL7, RPS18, RPS14* |
| 2 | Interleukin-2 signaling pathway | 110/728 | 3.38E-19 | 5.02E-17 | 0 | 110 | *VIM, BTN3A1, BTN3A2, BTN3A3, SOCS2, GZMK, CISH, CD69, GBP1, CCR2, DPP4, TAP1, TRIB2, GZMA, CD96, IL2RA, RPS6, S100A11, ITGAM, AIF1, CD52, DENND2D, PTGER2, CASP1, RNF144A, NELL2, FCER1G, NCR3, RPL21, S100A4, MEOX1, CCR5, CD40LG, CTSO, ADTRP, GZMM, MAL, VNN2, CD2, FYN, IL2RG, CTSS, APOBEC3G, IL4R, MT2A, CYP1A1, LITAF, VAMP5, RGS10, SELL, RBM3, CCR1, TNFRSF1B, IL2RB, NMT2, KCNN4, BTG1, LAT, HEMGN, PDCD4, MLLT3, CD27, LCP2, NKG7, AHNAK, GNLY, ETS1, ACP5, CX3CR1, RAB33A, TBCD, FLOT1, PDE7A, TNFRSF25, IRF1, IFIT1, CD300A, ITGB2, MDFIC, BCL2, ADAM19, TRIM21, TAGLN2, LTB, CCR7, NLRP1, PTPRC, CTSZ, SORL1, TXK, PARP8, TTN, SLA2, GATA3, SAMHD1, CCL5, AP3M2, IQGAP2, FCGBP, CXCL8, SPN, E2F3, TNFSF10, CAMK2N1, CTSH, SIT1, JAK3, PIM1, PRF1, EOMES* |
| 3 | Antigen processing and presentation | 27/54 | 7.67E-19 | 1.10E-16 | 0 | 27 | *HLA-DRA, HLA-DPA1, HLA-DPB1, PSMB9, HLA-E, CD74, HLA-DRB1, B2M, TAP1, PSME1, HLA-DRB5, HLA-DQA1, CIITA, HLA-DMB, CD8A, CTSS, PSMB8, HLA-B, HLA-F, CD4, HLA-DQB1, HLA-DOA, PSME2, TAP2, HLA-A, HLA-C, HSPA5* |
| 4 | Allograft rejection | 47/172 | 1.47E-18 | 2.03E-16 | 0 | 47 | *HLA-DRA, HLA-E, CD74, B2M, CCR2, TAP1, GZMA, CD96, IL2RA, KRT1, HLA-DQA1, GBP2, HLA-DMB, CD8A, CCR5, CD40LG, FYB1, RPS3A, CD2, IL2RG, CTSS, IL4R, RPL39, CAPG, CD3D, CCR1, IL2RB, CD4, HLA-DOA, CRTAM, ITGAL, TAP2, ST8SIA4, LCP2, HLA-A, RPL9, ETS1, DARS1, CD3E, ITGB2, LTB, CFP, PTPRC, CCL5, NLRP3, SIT1, PRF1* |

*[continued on next page]*

**Supplemental Table 1 | (h) (partial)** *[continued]*

| Group | Term | Overlap | P value | Adjusted P value | Up-regulated | Down-regulated | Genes |
|---|---|---|---|---|---|---|---|
| 5 | Interferon Gamma Response | 47/181 | 1.39E-17 | 1.80E-15 | 0 | 47 | *PSMB9, CD74, HLA-DRB1, B2M, CD69, TAP1, GZMA, PSME1, HLA-DQA1, CIITA, CASP1, SAMD9L, OAS2, TXNIP, IL4R, MT2A, SRI, VAMP5, PSMB8, HLA-B, XAF1, IL2RB, BTG1, NLRC5, PSME2, ST8SIA4, LCP2, HLA-A, ZBP1, IRF1, IFIT1, TRIM21, IL10RA, TRIM14, PNP, SLAMF7, OAS3, PARP12, CFH, SAMHD1, CCL5, TNFSF10, FGL2, ST3GAL5, PIM1, RTP4, SP110* |
| 6 | Cell adhesion molecules (CAMs) | 28/84 | 6.41E-14 | 6.94E-12 | 0 | 28 | *HLA-DRA, HLA-DPA1, HLA-DPB1, HLA-E, HLA-DRB1, CD226, ITGB1, ITGA4, ITGAM, HLA-DRB5, HLA-DQA1, HLA-DMB, CD8A, CD40LG, CD2, HLA-B, HLA-F, SELL, CD4, HLA-DQB1, HLA-DOA, ITGAL, HLA-A, PECAM1, ITGB2, HLA-C, PTPRC, SPN* |
| 7 | Immunoregulatory interactions between a lymphoid and a non-lymphoid cell | 26/77 | 3.63E-13 | 3.73E-11 | 0 | 26 | *HLA-E, B2M, CD226, IFITM1, CD96, ITGB1, ITGA4, LAIR1, NCR3, CD8A, CD40LG, CD3D, HLA-B, HLA-F, SELL, HCST, CRTAM, ITGAL, HLA-A, TYROBP, CD3E, CD300A, ITGB2, HLA-C, SLAMF7, CD200R1* |
| 8 | Cap-dependent translation initiation | 25/72 | 5.04E-13 | 4.92E-11 | 0 | 25 | *RPL35A, RPL30, RPL34, RPL23, RPL31, RPL21, RPL37, RPL23A, RPL11, RPL32, RPL27, RPL39, RPL38, RPL12, RPL4, RPL10A, RPL41, RPL37A, RPL9, RPL5, RPL24, RPL6, RPL19, UBA52, RPL7* |
| 9 | T cell receptor regulation of apoptosis | 76/529 | 3.50E-12 | 3.34E-10 | 0 | 76 | *VIM, RPS24, PSMB9, LGALS1, GBP1, IFITM1, CCR2, TAP1, IL2RA, PSME1, PTMA, RPL23, RPS29, S100A6, RPS20, CASP1, GADD45B, FCER1G, S100A4, RPL37, MCL1, CCR5, CD40LG, MAL, APOL3, RPS3A, CD2, CYBB, PSMB8, HLA-B, CCR1, TNFRSF1B, TRAF1, HLA-DQB1, RAC2, BTG1, ITGAL, RPL10A, PSME2, RPL41, RCBTB2, HSP90B1, TRAF5, PDE7A, HMGB1, TNFRSF25, CD3E, IRF1, ARHGDIB, CLIC5, ITGB2, BCL2, ATM, CDC42, RPL6, LTB, CCR7, NLRP1, PTPRC, RHOH, PNP, TUBB, HSPA5, GATA3, CCL5, IQGAP2, VIPR1, CXCL8, SPN, S100A10, NLRP3, CNBP, DYNLL1, PIM1, RPS14, SH3BGRL* |
| 10 | Viral myocarditis | 20/50 | 5.29E-12 | 4.93E-10 | 0 | 20 | *HLA-DRA, HLA-DPA1, HLA-DPB1, HLA-E, HLA-DRB1, HLA-DRB5, HLA-DQA1, HLA-DMB, CD40LG, FYN, HLA-B, HLA-F, HLA-DQB1, RAC2, HLA-DOA, ITGAL, HLA-A, ITGB2, HLA-C, PRF1* |

*[continued on next page]*

**Supplemental Table 1 | (h) (partial)** *[continued]*

| Group | Term | Overlap | P value | Adjusted P value | Up-regulated | Down-regulated | Genes |
|---|---|---|---|---|---|---|---|
| 11 | Interferon gamma signaling | 24/76 | 1.53E-11 | 1.28E-09 | 0 | 24 | *HLA-DRA, HLA-DPA1, HLA-DPB1, HLA-E, HLA-DRB1, B2M, GBP1, HLA-DRB5, HLA-DQA1, CIITA, GBP2, OAS2, GBP5, MT2A, HLA-B, HLA-F, HLA-DQB1, HLA-A, IRF1, TRIM21, HLA-C, CAMK2G, TRIM14, OAS3* |
| 12 | Immune system | 127/1169 | 9.49E-11 | 7.04E-09 | 0 | 127 | *HLA-DRA, HLA-DPA1, HLA-DPB1, PSMB9, HLA-E, SOCS2, CD74, IL32, TRIM69, LGALS3, CISH, HLA-DRB1, RPS27A, B2M, GBP1, CD226, IFITM1, CCR2, TAP1, CD96, IL2RA, ITGB1, ITGA4, PSME1, NEFL, ITGAM, HLA-DRB5, HLA-DQA1, CIITA, GBP2, TNFSF12, CASP1, HLA-DMB, LAIR1, TNFSF13B, FCER1G, NCR3, CD8A, OAS2, CD40LG, CTSO, GZMM, FYN, TLR5, IL2RG, TXNIP, CTSS, C5AR2, GBP5, P2RX7, MT2A, PTPRJ, CYBB, PSMB8, CD3D, CALM1, HLA-B, HLA-F, SELL, XAF1, TNFRSF1B, GRAP2, IL2RB, HCST, CD4, HLA-DQB1, CNKSR2, LAT, HLA-DOA, CRTAM, ITGAL, NLRC5, CD27, PSME2, TAP2, LCP2, HLA-A, TYROBP, SYNGAP1, MYLIP, HSP90B1, PEBP1, EDAR, ZBP1, HMGB1, TNFRSF25, CD3E, IRF1, ATP6V0E2, IFIT1, CD300A, ITGB2, BCL2, CDC42, TRIM21, HLA-C, CFL1, LTB, THEM4, CAMK2G, ARRB1, NLRP1, PTPRC, TRIM14, SLAMF7, RPS6KA5, ARPC2, TXK, ARPC3, HSPA5, OAS3, FGF9, UBA52, CFH, SAMHD1, UBE2F, FCN1, NUP37, NLRP3, CD200R1, CTSH, AIM2, SKP1, DYNLL1, JAK3, RPS6KA1, BTLA* |
| 13 | Phosphorylation of CD3 and TCR zeta chains | 12/19 | 1.14E-10 | 8.28E-09 | 0 | 12 | *HLA-DRA, HLA-DPA1, HLA-DPB1, HLA-DRB1, HLA-DRB5, HLA-DQA1, PTPRJ, CD3D, CD4, HLA-DQB1, CD3E, PTPRC* |
| 14 | Formation of the ternary complex, and subsequently, the 43S complex | 18/49 | 3.31E-10 | 2.29E-08 | 0 | 18 | *RPS24, RPS25, RPS27A, RPS12, RPS15A, RPS6, RPS29, RPS7, RPS21, RPS20, RPS23, RPS8, RPS13, RPS27, RPS3A, RPS11, RPS18, RPS14* |
| 15 | Asthma | 11/17 | 4.81E-10 | 3.16E-08 | 0 | 11 | *HLA-DRA, HLA-DPA1, HLA-DPB1, HLA-DRB1, HLA-DRB5, HLA-DQA1, HLA-DMB, FCER1G, CD40LG, HLA-DQB1, HLA-DOA* |
| 16 | Acute phase in atopic dermatitis | 14/30 | 7.29E-10 | 4.71E-08 | 0 | 14 | *IL2RA, MAF, FCER1G, CD40LG, FYN, IL2RG, IL4R, CD3D, IL2RB, CD4, CD3E, PTPRC, GATA3, JAK3* |

*[continued on next page]*

**Supplemental Table 1 | (h) (partial)** *[continued]*

| Group | Term | Overlap | P value | Adjusted P value | Up-regulated | Down-regulated | Genes |
|---|---|---|---|---|---|---|---|
| 17 | $CD8^+$ naive T-cell -> $CD4^+$ naive T-cell surface expression markers | 15/35 | 7.87E-10 | 5.01E-08 | 0 | 15 | *CD69, IL2RA, CCR5, CD40LG, IL4R, SELL, CD4, ITGAL, CD27, HLA-A, PECAM1, CCR7, PTPRC, BTLA, PRF1* |
| 18 | Hematopoietic cell lineage | 20/70 | 5.53E-09 | 3.12E-07 | 0 | 20 | *HLA-DRA, HLA-DPA1, HLA-DPB1, HLA-DRB1, IL2RA, ITGA4, ITGAM, HLA-DRB5, HLA-DQA1, HLA-DMB, CD8A, MS4A1, CD2, IL4R, CD3D, CD4, HLA-DQB1, HLA-DOA, CD3E, GP5* |
| 19 | Disease | 70/553 | 7.92E-09 | 4.35E-07 | 0 | 70 | *RPS24, RPS25, PSMB9, RPS27A, B2M, RPL35A, LYZ, RPS12, RPS15A, IGFBP4, PSME1, RPL30, RPL34, RPS6, RPL23, RPS29, RPL31, RPS7, RPS21, RPS20, RPS23, RPS8, RPS13, RPL21, RPL37, CCR5, RPL23A, RPL11, RPS27, RPL32, RPL27, RPS3A, FYN, APOBEC3G, RPL39, CYBB, RPL38, PSMB8, CALM1, RPL12, CD4, NMT2, IGFBP3, RPL4, RPL10A, PSME2, RPL41, HLA-A, RPL37A, HSP90B1, PPIA, RPL9, PDIA6, ATP6V0E2, RPL5, CDC42, RPL24, RPL6, THEM4, RPL19, HSPA5, FGF9, UBA52, RPS11, CXCL8, NUP37, RPL7, SKP1, RPS18, RPS14* |
| 20 | Interferon alpha response | 23/93 | 8.59E-09 | 4.65E-07 | 0 | 23 | *PSMB9, CD74, B2M, IFITM1, TAP1, PSME1, GBP2, CASP1, SAMD9L, LPAR6, TXNIP, IL4R, PSMB8, SELL, PSME2, IRF1, TRIM21, HLA-C, TRIM14, PARP12, LAMP3, RTP4, SP110* |

**Supplemental Table 1 | (i) (partial)** Pathway enrichment analysis of all upregulated EPA DEGs generated using *clusterProfiler* using 10 human pathway databases. Enriched pathways are shown with information on which group that term clusters into based on the Jaccard index > 0.70, pathway term, number of DEGs that overlap with that databases gene set for that pathway, p value, adjusted p value, number of DEGs in that pathway that were upregulated, number of DEGs in that pathway that were downregulated, and gene names of all DEGs included in that pathway. Only the top term of the 19 groups are shown here.

| Group | Term | Overlap | P value | Adjusted P value | Up-regulated | Down-regulated | Genes |
|---|---|---|---|---|---|---|---|
| 1 | NRF2 pathway | 20/86 | 6.08E-11 | 1.90E-07 | 20 | 0 | *NQO1, GCLC, MAFG, HMOX1, FTL, SLC5A3, SLC6A9, TXNRD1, SQSTM1, GSR, PRDX1, GCLM, G6PD, PGD, KEAP1, GSTP1, SLC39A7, SLC7A11, SLC6A6, SLC39A6* |
| 2 | Amino acid transport across the plasma membrane | 9/18 | 6.40E-09 | 6.65E-06 | 9 | 0 | *SLC7A5, SLC43A2, SLC7A1, SLC3A2, SLC38A2, SLC1A5, SLC1A4, SLC7A11, SLC6A6* |
| 3 | Glutamine in cancer metabolism | 9/24 | 1.40E-07 | 8.73E-05 | 9 | 0 | *SLC7A5, PSAT1, GCLC, SLC3A2, SLC1A5, PYCR1, GCLM, SLC7A11, PSPH* |
| 4 | Xenobiotic metabolism | 19/136 | 1.12E-06 | 0.00044 | 19 | 0 | *NQO1, GCLC, HMOX1, GABARAPL1, SLC1A5, ETFDH, AKR1C3, ARG2, PYCR1, GSR, PGD, EPHX1, UGDH, NPC1, SHMT2, SLC6A6, HES6, LONP1, PINK1* |
| 5 | mTORC1 signaling | 23/195 | 1.77E-06 | 0.00061 | 23 | 0 | *SLC7A5, PSAT1, GCLC, EDEM1, PHGDH, SLC1A5, TXNRD1, SQSTM1, MTHFD2, GSR, SLC1A4, PRDX1, DDIT3, G6PD, PPP1R15A, SLC7A11, SHMT2, SLC6A6, GLA, GAPDH, NAMPT, DDX39A, PSPH* |
| 6 | Metabolic reprogramming in colon cancer | 10/40 | 2.03E-06 | 0.00063 | 10 | 0 | *PSAT1, SLC1A5, TALDO1, PYCR1, G6PD, PGD, SHMT2, PKM, GAPDH, PSPH* |
| 7 | Oxidative stress in amyotrophic lateral sclerosis | 6/12 | 2.47E-06 | 0.00070 | 6 | 0 | *NQO1, GCLC, HMOX1, GSR, GCLM, KEAP1* |
| 8 | Unfolded protein response | 16/110 | 4.67E-06 | 0.00112 | 16 | 0 | *SLC7A5, PSAT1, HERPUD1, TARS1, IARS1, CHAC1, VEGFA, EDEM1, CEBPG, MTHFD2, SLC1A4, ATF4, CXXC1, SLC30A5, XPOT, EDC4* |
| 9 | Trans-sulfuration and one carbon metabolism | 8/28 | 7.44E-06 | 0.00166 | 8 | 0 | *PSAT1, GCLC, PHGDH, MTHFD2, MTHFD1L, GCLM, SHMT2, PSPH* |

*[continued on next page]*

**Supplemental Table 1 | (i) (partial)** *[continued]*

| Group | Term | Overlap | P value | Adjusted P value | Up-regulated | Down-regulated | Genes |
|---|---|---|---|---|---|---|---|
| 10 | Serine glycine biosynthesis | 4/5 | 1.08E-05 | 0.00207 | 4 | 0 | *PSAT1, PHGDH, SHMT2, PSPH* |
| 11 | Oxidative stress, all-trans-retinal and lipofuscin toxicity in AMD | 6/15 | 1.21E-05 | 0.00210 | 6 | 0 | *NQO1, HMOX1, VEGFA, GCLM, KEAP1, HIF1A* |
| 12 | SLC-mediated transmembrane transport | 19/164 | 1.84E-05 | 0.00302 | 19 | 0 | *SLC7A5, SLC43A2, SLC7A1, SLC3A2, SLC38A2, SLC5A3, SLC1A5, SLC6A9, CTNS, SLC12A7, SLCO3A1, SLC1A4, SLC35A2, NUP153, SLC39A7, SLC7A11, SLC6A6, SLC30A5, SLC39A6* |
| 13 | Glutathione metabolism | 8/38 | 8.33E-05 | 0.01039 | 8 | 0 | *ODC1, GCLC, CHAC1, GSR, GCLM, G6PD, PGD, GSTP1* |
| 14 | Amino acid biosynthesis and interconversion (transamination) | 5/14 | 0.00013 | 0.01424 | 5 | 0 | *PSAT1, PHGDH, PYCR1, GPT2, PSPH* |
| 15 | mTOR signaling activation by amino acids | 8/41 | 0.00015 | 0.01581 | 8 | 0 | *SLC7A5, SLC3A2, SLC1A5, FNIP1, SESN2, FLCN, ATF4, PPP1R15A* |
| 16 | Reactive oxygen species pathway | 8/45 | 0.00029 | 0.02914 | 8 | 0 | *NQO1, GCLC, FTL, TXNRD1, GSR, PRDX1, GCLM, G6PD* |
| 17 | Ferroptosis | 7/35 | 0.00033 | 0.03089 | 7 | 0 | *GCLC, HMOX1, SLC3A2, FTL, SAT2, GCLM, SLC7A11* |
| 18 | Protein nuclear import and export | 5/17 | 0.00036 | 0.03293 | 5 | 0 | *XPO1, NXF1, RCC1, NUP153, XPOT* |
| 19 | Metabolic reprogramming in cancer: overview | 9/59 | 0.00040 | 0.03507 | 9 | 0 | *PSAT1, PHGDH, SLC1A5, PYCR1, SHMT2, PKM, GAPDH, HIF1A, PSPH* |

**Supplemental Table 1 | (j) (partial)** Known motif analysis on promotors of down versus upregulated EPA ATAC peaks. Enriched transcription factors are shown in order of significance. Enrichment of transcription factor binding motifs was performed using HOMER. Information on rank, motif, name of transcription factor, p value, log p value, q value (Benjamini), number of target sequences with motif, number of background sequences with motif, percent of targets sequences with motif, and percent of background sequences with motif. Top 20 significant transcription factors are shown here.

| Rank | Motif | Name | P value | q value (Benjamini) | # TS with Motif | # BG with Motif | % TS with Motif | % BG with Motif |
|---|---|---|---|---|---|---|---|---|
| 1 |  | CTCF | 1.00E-40 | 0 | 41.00 | 0.90 | 3.40% | 0.14% |
| 2 |  | BORIS | 1.00E-32 | 0 | 35.00 | 1.00 | 2.90% | 0.15% |
| 3 |  | OCT:OCT | 1.00E-22 | 0 | 172.0 | 42.90 | 14.27% | 6.38% |
| 4 |  | KLF10 | 1.00E-15 | 0 | 110.0 | 26.30 | 9.13% | 3.92% |
| 5 |  | GRE | 1.00E-13 | 0 | 35.00 | 4.80 | 2.90% | 0.72% |
| 6 |  | X-box | 1.00E-13 | 0 | 19.00 | 1.60 | 1.58% | 0.24% |
| 7 |  | GRE | 1.00E-09 | 0 | 21.00 | 2.90 | 1.74% | 0.43% |
| 8 |  | ARE | 1.00E-09 | 0 | 29.00 | 4.30 | 2.41% | 0.64% |
| 9 |  | GATA3 | 1.00E-09 | 0 | 15.00 | 1.70 | 1.24% | 0.26% |
| 10 |  | ETS:RUNX | 1.00E-08 | 0 | 14.00 | 0.60 | 1.16% | 0.10% |

*[continued on next page]*

**Supplemental Table 1 | (j) (partial)** *[continued]*

| Rank | Motif | Name | P value | q value (Benjamini) | # TS with Motif | # BG with Motif | % TS with Motif | % BG with Motif |
|---|---|---|---|---|---|---|---|---|
| 11 |  | RFX1 | 1.00E-07 | 0 | 27.00 | 4.40 | 2.24% | 0.66% |
| 12 |  | ETV2 | 1.00E-07 | 0 | 111.0 | 36.30 | 9.21% | 5.40% |
| 13 |  | RFX2 | 1.00E-07 | 0 | 13.00 | 1.00 | 1.08% | 0.15% |
| 14 |  | ZFP57 | 1.00E-07 | 0 | 13.00 | 1.60 | 1.08% | 0.24% |
| 15 |  | BRN1 | 1.00E-06 | 0 | 68.00 | 19.70 | 5.64% | 2.94% |
| 16 |  | GATA2 | 1.00E-06 | 0 | 95.00 | 32.00 | 7.88% | 4.75% |
| 17 |  | ETV4 | 1.00E-06 | 0 | 101.0 | 34.60 | 8.38% | 5.15% |
| 18 |  | PSE | 1.00E-05 | 0.0001 | 97.00 | 33.50 | 8.05% | 4.98% |
| 19 |  | PGR | 1.00E-05 | 0.0001 | 43.00 | 11.80 | 3.57% | 1.75% |
| 20 |  | PU.1 | 1.00E-05 | 0.0001 | 58.00 | 17.30 | 4.81% | 2.58% |

**Supplemental Table 1 | (k) (partial)** Known motif analysis on promotors of up versus downregulated EPA ATAC peaks. Enriched transcription factors are shown in order of significance. Enrichment of transcription factor binding motifs was performed using HOMER. Information on rank, motif, name of transcription factor, p value, log p value, q value (Benjamini), number of target sequences with motif, number of background sequences with motif, percent of targets sequences with motif, and percent of background sequences with motif. Top 20 significant transcription factors are shown here.

| Rank | Motif | Name | P value | q value (Benjamini) | # TS with Motif | # BG with Motif | % TS with Motif | % BG with Motif |
|---|---|---|---|---|---|---|---|---|
| 1 |  | AP-2α | 1.00E-12 | 0 | 74.00 | 34.10 | 7.91% | 3.08% |
| 2 |  | THRb | 1.00E-08 | 0 | 438.0 | 413.5 | 46.84% | 37.39% |
| 3 |  | E2F4 | 1.00E-08 | 0 | 14.00 | 3.00 | 1.50% | 0.27% |
| 4 |  | OCT4:SOX17 | 1.00E-05 | 0.0002 | 17.00 | 5.30 | 1.82% | 0.48% |
| 5 |  | E2F1 | 1.00E-05 | 0.0003 | 8.00 | 0.00 | 0.86% | 0.00% |
| 6 |  | ZIC | 1.00E-05 | 0.0005 | 88.00 | 64.50 | 9.41% | 5.84% |
| 7 |  | PBX3 | 1.00E-05 | 0.0005 | 21.00 | 8.90 | 2.25% | 0.81% |
| 8 |  | AR | 1.00E-05 | 0.0005 | 399.0 | 396.4 | 42.67% | 35.85% |
| 9 |  | ZNF136 | 1.00E-04 | 0.0007 | 12.00 | 3.60 | 1.28% | 0.32% |
| 10 |  | REV-ERB | 1.00E-04 | 0.0034 | 19.00 | 8.80 | 2.03% | 0.79% |

*[continued on next page]*

**Supplemental Table 1 | (k) (partial)** *[continued]*

| Rank | Motif | Name | P value | q value (Benjamini) | # TS with Motif | # BG with Motif | % TS with Motif | % BG with Motif |
|---|---|---|---|---|---|---|---|---|
| 11 |  | STAT4 | 1.00E-03 | 0.0071 | 98.00 | 80.30 | 10.48% | 7.26% |
| 12 |  | TR4 | 1.00E-03 | 0.0088 | 6.00 | 1.30 | 0.64% | 0.12% |
| 13 |  | GLI3 | 1.00E-03 | 0.0088 | 15.00 | 6.70 | 1.60% | 0.61% |
| 14 |  | MYB | 1.00E-03 | 0.0088 | 141.0 | 125.2 | 15.08% | 11.32% |
| 15 |  | MYNN | 1.00E-03 | 0.0088 | 27.00 | 16.00 | 2.89% | 1.44% |
| 16 |  | ZSCAN22 | 1.00E-03 | 0.0088 | 10.00 | 3.90 | 1.07% | 0.35% |
| 17 |  | THRa | 1.00E-03 | 0.0092 | 72.00 | 56.50 | 7.70% | 5.11% |
| 18 |  | TCF7 | 1.00E-03 | 0.0092 | 35.00 | 22.20 | 3.74% | 2.01% |
| 19 |  | TGIF1 | 1.00E-03 | 0.0101 | 318.0 | 320.4 | 34.01% | 28.98% |
| 20 |  | HNF4a | 1.00E-03 | 0.0118 | 49.00 | 35.40 | 5.24% | 3.20% |

**Supplemental Table 1 | (l) (partial)** Pathway enrichment analysis of all downregulated OA DEGs generated using *clusterProfiler* using 10 human pathway databases. Enriched pathways are shown with information on which group that term clusters into based on the Jaccard index > 0.70, pathway term, number of DEGs that overlap with that databases gene set for that pathway, p value, adjusted p value, number of DEGs in that pathway that were upregulated, number of DEGs in that pathway that were downregulated, and gene names of all DEGs included in that pathway. Only the top term of the 11 groups are shown here.

| Group | Term | Overlap | P value | Adjusted P value | Up-regulated | Down-regulated | Genes |
|---|---|---|---|---|---|---|---|
| 1 | Prion disease pathway | 3/33 | 9.94E-06 | 0.00264 | 0 | 3 | *HSP90B1, HSPA5, PDIA3* |
| 2 | Co-translational ER protein import | 2/6 | 2.48E-05 | 0.00264 | 0 | 2 | *HSP90B1, HSPA5* |
| 3 | Endogenous peptide antigen presentation | 2/6 | 2.48E-05 | 0.00264 | 0 | 2 | *HSPA5, PDIA3* |
| 4 | Protein folding | 2/13 | 0.00013 | 0.00401 | 0 | 2 | *HSP90B1, HSP90AA1* |
| 5 | Electron transport chain (OXPHOS system in mitochondria) | 3/87 | 0.00019 | 0.00534 | 0 | 3 | *NDUFA12, NDUFB4, ATP5F1C* |
| 6 | ER stress (unfolded protein response) | 2/31 | 0.00076 | 0.01277 | 0 | 2 | *HSPA5, HSP90AA1* |
| 7 | Proteins involved in myocardial ischemia | 3/161 | 0.00113 | 0.01639 | 0 | 3 | *TMSB4X, TXNIP, HSP90AA1* |
| 8 | Apoptotic keratinocytes clearance recession in systemic lupus erythematosus | 2/38 | 0.00114 | 0.01639 | 0 | 2 | *HSP90B1, TXNIP* |
| 9 | Complex I biogenesis | 2/49 | 0.00189 | 0.02438 | 0 | 2 | *NDUFA12, NDUFB4* |
| 10 | Response to elevated platelet cytosolic calcium | 2/56 | 0.00246 | 0.02878 | 0 | 2 | *TMSB4X, HSPA5* |
| 11 | T cell receptor regulation of apoptosis | 4/529 | 0.00414 | 0.03977 | 0 | 4 | *HSP90B1, HSPA5, ARHGDIB, HSP90AA1* |

**Supplemental Table 1 | (m) (partial)** Pathway enrichment analysis of all upregulated OA DEGs generated using *clusterProfiler* using 10 human pathway databases. Enriched pathways are shown with information on which group that term clusters into based on the Jaccard index > 0.70, pathway term, number of DEGs that overlap with that databases gene set for that pathway, p value, adjusted p value, number of DEGs in that pathway that were upregulated, number of DEGs in that pathway that were downregulated, and gene names of all DEGs included in that pathway. Only the top term of the first 20 groups are shown here.

| Group | Term | Overlap | P value | Adjusted P value | Up-regulated | Down-regulated | Genes |
|---|---|---|---|---|---|---|---|
| 1 | Lipid and lipoprotein metabolism | 13/372 | 2.86E-09 | 5.90E-07 | 13 | 0 | *CPT1A, SLC25A20, ACADVL, LPCAT1, DHCR24, FASN, SREBF2, LDLR, HMGCR, UGCG, SPTLC2, KDSR, HMGCS1* |
| 2 | SREBF and miR-33 in cholesterol and lipid homeostasis | 5/15 | 3.57E-09 | 5.90E-07 | 5 | 0 | *FASN, SREBF2, LDLR, HMGCR, HMGCS1* |
| 3 | Fatty acid, triacylglycerol, and ketone body metabolism | 8/148 | 1.90E-07 | 1.88E-05 | 8 | 0 | *CPT1A, SLC25A20, ACADVL, LPCAT1, FASN, SREBF2, HMGCR, HMGCS1* |
| 4 | Fatty acid metabolism | 7/133 | 1.45E-06 | 8.99E-05 | 7 | 0 | *CPT1A, ACADVL, DHCR24, FASN, ACAA2, ETFDH, HMGCS1* |
| 5 | Cholesterol biosynthesis | 4/23 | 2.61E-06 | 0.00013 | 4 | 0 | *DHCR24, SREBF2, HMGCR, HMGCS1* |
| 6 | srebp control of lipid synthesis | 3/7 | 2.68E-06 | 0.00013 | 3 | 0 | *SREBF2, LDLR, HMGCS1* |
| 7 | mTORC1 signaling | 7/194 | 1.77E-05 | 0.00063 | 7 | 0 | *DHCR24, LDLR, HMGCR, SQSTM1, HMGCS1, PPP1R15A, INSIG1* |
| 8 | Androgen response | 5/86 | 3.30E-05 | 0.00102 | 5 | 0 | *DHCR24, HMGCR, ABHD2, HMGCS1, INSIG1* |
| 9 | Mitochondrial LC-fatty acid beta-oxidation | 3/16 | 4.17E-05 | 0.00122 | 3 | 0 | *CPT1A, SLC25A20, ACADVL* |
| 10 | TNF-α signaling via NF-κB | 6/169 | 8.24E-05 | 0.00227 | 6 | 0 | *SNN, LDLR, SQSTM1, B4GALT5, KLF10, PPP1R15A* |
| 11 | HNF3B pathway | 3/23 | 0.00013 | 0.00263 | 3 | 0 | *CPT1A, ACADVL, HMGCS1* |

*[continued on next page]*

**Supplemental Table 1 | (m) (partial)** *[continued]*

| Group | Term | Overlap | P value | Adjusted P value | Up-regulated | Down-regulated | Genes |
|---|---|---|---|---|---|---|---|
| 12 | Proteins involved in non-alcoholic fatty liver disease | 5/115 | 0.00013 | 0.00263 | 5 | 0 | *CPT1A, FASN, SREBF2, LDLR, INSIG1* |
| 13 | Ceramide *de novo* biosynthesis | 2/6 | 0.00028 | 0.00479 | 2 | 0 | *SPTLC2, KDSR* |
| 14 | Fatty acid metabolism | 3/33 | 0.00039 | 0.00563 | 3 | 0 | *CPT1A, ACADVL, ACAA2* |
| 15 | Import of palmitoyl-CoA into the mitochondrial matrix | 2/7 | 0.00039 | 0.00563 | 2 | 0 | *CPT1A, SLC25A20* |
| 16 | Mevalonate pathway | 2/7 | 0.00039 | 0.00563 | 2 | 0 | *HMGCR, HMGCS1* |
| 17 | Estrogen response early | 5/147 | 0.00042 | 0.00591 | 5 | 0 | *FASN, FAM102A, ABHD2, UGCG, KLF10* |
| 18 | Synthesis of UDP-N-acetyl-glucosamine | 2/8 | 0.00051 | 0.00688 | 2 | 0 | *RENBP, AMDHD2* |
| 19 | Sphingolipid metabolism | 3/40 | 0.00068 | 0.00869 | 3 | 0 | *UGCG, SPTLC2, KDSR* |
| 20 | Oncostatin M | 5/167 | 0.00075 | 0.00883 | 5 | 0 | *DHCR24, LDLR, HMGCR, HMGCS1, KLF10* |

**Supplemental Table 1 | (n)** Pathway enrichment analysis of all downregulated PA DEGs generated using *clusterProfiler* using 10 human pathway databases. Enriched pathways are shown with information on which group that term clusters into based on the Jaccard index > 0.70, pathway term, number of DEGs that overlap with that databases gene set for that pathway, p value, adjusted p value, number of DEGs in that pathway that were upregulated, number of DEGs in that pathway that were downregulated, and gene names of all DEGs included in that pathway.

| Group | Term | Overlap | P value | Adjusted P value | Up-regulated | Down-regulated | Genes |
|---|---|---|---|---|---|---|---|
| 1 | Cholesterol biosynthesis | 2/10 | 7.41E-05 | 0.01047 | 0 | 2 | *HMGCR, SQLE* |
| 2 | Cholesterol biosynthesis pathway | 2/15 | 0.00017 | 0.01047 | 0 | 2 | *HMGCR, SQLE* |
| 3 | Statin pathway | 2/16 | 0.00020 | 0.01047 | 0 | 2 | *HMGCR, SQLE* |
| 4 | Statin pathway | 2/16 | 0.00020 | 0.01047 | 0 | 2 | *HMGCR, SQLE* |
| 5 | Cholesterol biosynthesis | 2/22 | 0.00038 | 0.01255 | 0 | 2 | *HMGCR, SQLE* |
| 6 | Cholesterol biosynthesis | 2/23 | 0.00041 | 0.01255 | 0 | 2 | *HMGCR, SQLE* |
| 7 | Superpathway of cholesterol biosynthesis | 2/23 | 0.00041 | 0.01255 | 0 | 2 | *HMGCR, SQLE* |
| 8 | Activation of gene expression by SREBF (SREBP) | 2/42 | 0.00138 | 0.03683 | 0 | 2 | *HMGCR, SQLE* |

**Supplemental Table 1 | (o) (partial)** All significant pathway enrichment analysis of all upregulated PA DEGs generated using *clusterProfiler* using 10 human pathway databases. Enriched pathways are shown with information on which group that term clusters into based on the Jaccard index > 0.70, pathway term, number of DEGs that overlap with that databases gene set for that pathway, p value, adjusted p value, number of DEGs in that pathway that were upregulated, number of DEGs in that pathway that were downregulated, and gene names of all DEGs included in that pathway. Only the top term of the first 20 groups are shown here.

| Group | Term | Overlap | P value | Adjusted P value | Up-regulated | Down-regulated | Genes |
|---|---|---|---|---|---|---|---|
| 1 | Estrogen deficiency in female obesity | 3/6 | 6.12E-08 | 1.44E-05 | 3 | 0 | *SREBF1, SCD, ACACA* |
| 2 | Fatty acid, triacylglycerol, and ketone body metabolism | 6/175 | 1.37E-07 | 1.44E-05 | 6 | 0 | *CPT1A, SLC25A20, ACADVL, SREBF1, SCD, ACACA* |
| 3 | Import of palmitoyl-CoA into the mitochondrial matrix | 3/10 | 3.66E-07 | 2.52E-05 | 3 | 0 | *CPT1A, SLC25A20, ACACA* |
| 4 | Mitochondrial LC-fatty acid beta-oxidation | 3/16 | 1.70E-06 | 6.94E-05 | 3 | 0 | *CPT1A, SLC25A20, ACADVL* |
| 5 | Ghrelin pathway | 3/19 | 2.93E-06 | 9.31E-05 | 3 | 0 | *SREBF1, ABCG1, ACACA* |
| 6 | Fatty acid biosynthesis | 3/22 | 4.64E-06 | 0.00011 | 3 | 0 | *ACAA2, SCD, ACACA* |
| 7 | Liver X receptor pathway | 2/5 | 2.28E-05 | 0.00028 | 2 | 0 | *SREBF1, SCD* |
| 8 | Import of palmitoyl-CoA into the mitochondrial matrix | 2/7 | 4.77E-05 | 0.00055 | 2 | 0 | *CPT1A, SLC25A20* |
| 9 | reversal of insulin resistance by leptin | 2/8 | 6.36E-05 | 0.00063 | 2 | 0 | *CPT1A, ACACA* |
| 10 | AMPK related catabolism deceleration in glucose insufficiency | 2/8 | 6.36E-05 | 0.00063 | 2 | 0 | *SREBF1, ACACA* |
| 11 | HNF3B pathway | 2/23 | 0.00057 | 0.00345 | 2 | 0 | *CPT1A, ACADVL* |
| 12 | RORA activates circadian expression | 2/25 | 0.00067 | 0.00400 | 2 | 0 | *CPT1A, SREBF1* |
| 13 | Fatty acyl-CoA biosynthesis | 2/31 | 0.00103 | 0.00580 | 2 | 0 | *SCD, ACACA* |

*[continued on next page]*

**Supplemental Table 1 | (o) (partial)** *[continued]*

| Group | Term | Overlap | P value | Adjusted P value | Up-regulated | Down-regulated | Genes |
|---|---|---|---|---|---|---|---|
| 14 | Circadian rhythm related genes | 3/135 | 0.00109 | 0.00599 | 3 | 0 | *CPT1A, SREBF1, KLF10* |
| 15 | PPAR signaling pathway | 2/40 | 0.00172 | 0.00895 | 2 | 0 | *CPT1A, SCD* |
| 16 | Activation of chaperones by IRE1 alpha | 2/45 | 0.00217 | 0.01072 | 2 | 0 | *ACADVL, HYOU1* |
| 17 | Oleate biosynthesis | 1/3 | 0.00470 | 0.01975 | 1 | 0 | *SCD* |
| 18 | Metabolism | 6/1142 | 0.00520 | 0.02155 | 6 | 0 | *CPT1A, ACADVL, LPCAT3, ABCG1, ACAA2, ACACA* |
| 19 | Beta-oxidation of myristoyl-CoA to lauroyl-CoA | 1/4 | 0.00626 | 0.02451 | 1 | 0 | *ACADVL* |
| 20 | VEGFR -> CTNND signaling | 1/4 | 0.00626 | 0.02451 | 1 | 0 | *COL18A1* |

**Supplemental Table 1 | (p)** Known motif analysis on promotors of down versus upregulated OA ATAC peaks. All enriched transcription factors are shown in order of significance. Enrichment of transcription factor binding motifs was performed using HOMER. Information on rank, motif, name of transcription factor, p value, log p value, q value (Benjamini), number of target sequences with motif, number of background sequences with motif, percent of targets sequences with motif, and percent of background sequences with motif.

| Rank | Motif | Name | P value | q value (Benjamini) | # TS with Motif | # BG with Motif | % TS with Motif | % BG with Motif |
|---|---|---|---|---|---|---|---|---|
| 1 |  | ZNF41 | 1.00E-02 | 0.9003 | 5.00 | 6.40 | 0.54% | 0.10% |
| 2 |  | RAR:RXR | 1.00E-02 | 1 | 5.00 | 8.30 | 0.54% | 0.13% |
| 3 |  | WT1 | 1.00E-02 | 1 | 48.00 | 228.8 | 5.15% | 3.60% |

**Supplemental Table 1 | (q) (partial)** Known motif analysis on promotors of up versus downregulated OA ATAC peaks. Enriched transcription factors are shown in order of significance. Enrichment of transcription factor binding motifs was performed using HOMER. Information on rank, motif, name of transcription factor, p value, log p value, q value (Benjamini), number of target sequences with motif, number of background sequences with motif, percent of targets sequences with motif, and percent of background sequences with motif. Top 23 significant transcription factors are shown here.

| Rank | Motif | Name | P value | q value (Benjamini) | # TS with Motif | # BG with Motif | % TS with Motif | % BG with Motif |
|---|---|---|---|---|---|---|---|---|
| 1 |  | Twist | 1.00E-20 | 0 | 49.00 | 2.70 | 1.28% | 0.30% |
| 2 |  | ZIC3 | 1.00E-20 | 0 | 217.0 | 25.40 | 5.68% | 2.85% |
| 3 |  | GLI2 | 1.00E-20 | 0 | 109.0 | 9.00 | 2.85% | 1.01% |
| 4 |  | PAX5 | 1.00E-17 | 0 | 33.00 | 1.80 | 0.86% | 0.20% |
| 5 |  | EHF | 1.00E-16 | 0 | 456.0 | 71.30 | 11.94% | 8.01% |
| 6 |  | GFY | 1.00E-11 | 0 | 26.00 | 0.00 | 0.68% | 0.00% |
| 7 |  | Duxbl | 1.00E-11 | 0 | 25.00 | 1.20 | 0.65% | 0.13% |
| 8 |  | ZSCAN22 | 1.00E-10 | 0 | 35.00 | 2.50 | 0.92% | 0.28% |
| 9 |  | RXR | 1.00E-10 | 0 | 442.0 | 75.80 | 11.58% | 8.51% |
| 10 |  | STAT4 | 1.00E-10 | 0 | 320.0 | 51.80 | 8.38% | 5.82% |
| 11 |  | AP-2α | 1.00E-10 | 0 | 313.0 | 50.30 | 8.20% | 5.65% |

*[continued on next page]*

**Supplemental Table 1 | (q) (partial)** *[continued]*

| Rank | Motif | Name | P value | q value (Benjamini) | # TS with Motif | # BG with Motif | % TS with Motif | % BG with Motif |
|---|---|---|---|---|---|---|---|---|
| 12 |  | OCT4:SOX17 | 1.00E-09 | 0 | 48.00 | 4.50 | 1.26% | 0.50% |
| 13 |  | PTF1A | 1.00E-09 | 0 | 1198.0 | 240.9 | 31.38% | 27.06% |
| 14 |  | ZNF692 | 1.00E-08 | 0 | 93.00 | 11.50 | 2.44% | 1.29% |
| 15 |  | PPARα | 1.00E-08 | 0 | 412.0 | 72.20 | 10.79% | 8.11% |
| 16 |  | ELF4 | 1.00E-08 | 0 | 351.0 | 60.70 | 9.19% | 6.82% |
| 17 |  | DMC1 | 1.00E-08 | 0 | 21.00 | 0.00 | 0.55% | 0.00% |
| 18 |  | RUNX2 | 1.00E-08 | 0 | 370.0 | 64.60 | 9.69% | 7.26% |
| 19 |  | Nur77 | 1.00E-07 | 0 | 59.00 | 6.20 | 1.55% | 0.69% |
| 20 |  | ETS1 | 1.00E-07 | 0 | 118.0 | 16.70 | 3.09% | 1.87% |
| 21 |  | SMAD4 | 1.00E-07 | 0 | 600.0 | 113.1 | 15.72% | 12.70% |
| 22 |  | PU.1 | 1.00E-07 | 0 | 188.0 | 30.00 | 4.92% | 3.37% |
| 23 |  | IRF8 | 1.00E-07 | 0 | 70.00 | 8.30 | 1.83% | 0.93% |

**Supplemental Table 1 | (r)** Known motif analysis on promotors of down versus upregulated PA ATAC peaks. All enriched transcription factors are shown in order of significance. Enrichment of transcription factor binding motifs was performed using HOMER. Information on rank, motif, name of transcription factor, p value, log p value, q value (Benjamini), number of target sequences with motif, number of background sequences with motif, percent of targets sequences with motif, and percent of background sequences with motif.

| Rank | Motif | Name | P value | q value (Benjamini) | # TS with Motif | # BG with Motif | % TS with Motif | % BG with Motif |
|---|---|---|---|---|---|---|---|---|
| 1 |  | IRF8 | 1.00E-04 | 0.022 | 25.00 | 27.00 | 4.62% | 1.96% |
| 2 |  | PBX3 | 1.00E-03 | 0.143 | 18.00 | 19.10 | 3.33% | 1.38% |
| 3 |  | NFkB | 1.00E-03 | 0.143 | 4.00 | 0.80 | 0.74% | 0.06% |
| 4 |  | ZNF382 | 1.00E-03 | 0.143 | 4.00 | 0.90 | 0.74% | 0.06% |
| 5 |  | ETS:E-box | 1.00E-02 | 0.143 | 11.00 | 9.20 | 2.03% | 0.67% |
| 6 |  | GATA2 | 1.00E-02 | 0.147 | 48.00 | 79.60 | 8.87% | 5.77% |
| 7 |  | NKX3-2 | 1.00E-02 | 0.185 | 174.0 | 369.4 | 32.16% | 26.78% |
| 8 |  | GATA3 | 1.00E-02 | 0.234 | 9.00 | 8.20 | 1.66% | 0.60% |
| 9 |  | IRF2 | 1.00E-02 | 0.234 | 9.00 | 8.80 | 1.66% | 0.64% |
| 10 |  | p63 | 1.00E-02 | 0.234 | 25.00 | 37.00 | 4.62% | 2.68% |
| 11 |  | ZNF264 | 1.00E-02 | 0.234 | 34.00 | 54.70 | 6.28% | 3.97% |

*[continued on next page]*

**Supplemental Table 1 | (r)** *[continued]*

| Rank | Motif | Name | P value | q value (Benjamini) | # TS with Motif | # BG with Motif | % TS with Motif | % BG with Motif |
|---|---|---|---|---|---|---|---|---|
| 12 |  | ZNF317 | 1.00E-02 | 0.234 | 6.00 | 5.00 | 1.11% | 0.36% |
| 13 |  | GATA4 | 1.00E-02 | 0.234 | 67.00 | 125.9 | 12.38% | 9.12% |
| 14 |  | GATA1 | 1.00E-02 | 0.237 | 41.00 | 70.20 | 7.58% | 5.09% |
| 15 |  | IRF3 | 1.00E-02 | 0.242 | 20.00 | 28.20 | 3.70% | 2.04% |
| 16 |  | TLX | 1.00E-02 | 0.253 | 25.00 | 38.70 | 4.62% | 2.80% |
| 17 |  | FOXM1 | 1.00E-02 | 0.253 | 72.00 | 139.5 | 13.31% | 10.11% |
| 18 |  | NFY | 1.00E-02 | 0.253 | 48.00 | 86.70 | 8.87% | 6.28% |
| 19 |  | ELF4 | 1.00E-02 | 0.253 | 53.00 | 97.10 | 9.80% | 7.04% |

**Supplemental Table 1 | (s) (partial)** Known motif analysis on promotors of up versus downregulated PA ATAC peaks. All enriched transcription factors are shown in order of significance. Enrichment of transcription factor binding motifs was performed using HOMER. Information on rank, motif, name of transcription factor, p value, log p value, q value (Benjamini), number of target sequences with motif, number of background sequences with motif, percent of targets sequences with motif, and percent of background sequences with motif. Top 20 significant transcription factors are shown here.

| Rank | Motif | Name | P value | q value (Benjamini) | # TS with Motif | # BG with Motif | % TS with Motif | % BG with Motif |
|---|---|---|---|---|---|---|---|---|
| 1 |  | PITX1 | 1.00E-09 | 0 | 30.00 | 3.10 | 2.16% | 0.57% |
| 2 |  | ZBTB12 | 1.00E-08 | 0 | 63.00 | 11.80 | 4.54% | 2.19% |
| 3 |  | HOXC9 | 1.00E-07 | 0 | 95.00 | 20.30 | 6.84% | 3.75% |
| 4 |  | Pdx1 | 1.00E-07 | 0 | 183.0 | 47.10 | 13.17% | 8.74% |
| 5 |  | Nur77 | 1.00E-07 | 0 | 22.00 | 2.70 | 1.58% | 0.49% |
| 6 |  | HOXA1 | 1.00E-05 | 0.0001 | 37.00 | 6.90 | 2.66% | 1.27% |
| 7 |  | DR4 | 1.00E-05 | 0.0003 | 32.00 | 5.20 | 2.30% | 0.97% |
| 8 |  | CHOP | 1.00E-04 | 0.0008 | 46.00 | 9.60 | 3.31% | 1.77% |
| 9 |  | REV-ERB | 1.00E-04 | 0.0009 | 22.00 | 3.70 | 1.58% | 0.68% |
| 10 |  | EBF | 1.00E-04 | 0.0012 | 17.00 | 2.90 | 1.22% | 0.53% |

*[continued on next page]*

**Supplemental Table 1 | (s) (partial)** *[continued]*

| Rank | Motif | Name | P value | q value (Benjamini) | # TS with Motif | # BG with Motif | % TS with Motif | % BG with Motif |
|---|---|---|---|---|---|---|---|---|
| 11 |  | COUP-TFII | 1.00E-04 | 0.0012 | 230.0 | 69.50 | 16.56% | 12.88% |
| 12 |  | IRF:BATF | 1.00E-04 | 0.0033 | 16.00 | 2.50 | 1.15% | 0.46% |
| 13 |  | MEF2B | 1.00E-03 | 0.0036 | 171.0 | 51.00 | 12.31% | 9.45% |
| 14 |  | PBX2 | 1.00E-03 | 0.0037 | 153.0 | 44.30 | 11.02% | 8.21% |
| 15 |  | PAX5 | 1.00E-03 | 0.0046 | 53.00 | 12.80 | 3.82% | 2.38% |
| 16 |  | ZNF415 | 1.00E-03 | 0.0067 | 75.00 | 19.60 | 5.40% | 3.62% |
| 17 |  | SOX9 | 1.00E-03 | 0.0067 | 112.0 | 31.20 | 8.06% | 5.79% |
| 18 |  | STAT4 | 1.00E-03 | 0.0067 | 130.0 | 37.40 | 9.36% | 6.92% |
| 19 |  | COUP-TFII | 1.00E-03 | 0.0067 | 248.0 | 78.20 | 17.85% | 14.50% |
| 20 |  | PBX1 | 1.00E-03 | 0.0074 | 10.00 | 0.00 | 0.72% | 0.00% |